

Precision Theory for Heavy Flavour Physics

Mikołaj Misiak

University of Warsaw

“Prospecting for New Physics through Flavor, Dark Matter, and Machine Learning”,
Aspen Center for Physics, March 26th-31st, 2023

1. Introduction
2. $b \rightarrow s\ell^+\ell^-$ transitions and $R_{D^{(*)}}$
3. Update on $B_{s(d)} \rightarrow \mu^+\mu^-$
4. $\mathcal{B}(B \rightarrow X_s\gamma)$ – perturbative and non-perturbative contributions
5. Precision determinations of V_{cb} from inclusive $B \rightarrow X\ell\bar{\nu}$
6. Summary

In new physics models where all the BSM particles have masses $m_1 \equiv \Lambda \leq m_2 \leq m_3 \dots m_n$, with $\Lambda \gg m_t$, and interact in a perturbative manner, the Standard Model Effective Field Theory (SMEFT) is a useful tool for describing physics phenomena at energy scales well below Λ .

In new physics models where all the BSM particles have masses $m_1 \equiv \Lambda \leq m_2 \leq m_3 \dots m_n$, with $\Lambda \gg m_t$, and interact in a perturbative manner, the Standard Model Effective Field Theory (SMEFT) is a useful tool for describing physics phenomena at energy scales well below Λ .

$$\mathcal{L}_{\text{SMEFT}} = \mathcal{L}_{\text{SM}} + \frac{1}{\Lambda} \sum_k C_k^{(5)}(\mu) Q_k^{(5)} + \frac{1}{\Lambda^2} \sum_k C_k^{(6)}(\mu) Q_k^{(6)} + \mathcal{O}\left(\frac{1}{\Lambda^3}\right).$$

In new physics models where all the BSM particles have masses $m_1 \equiv \Lambda \leq m_2 \leq m_3 \dots m_n$, with $\Lambda \gg m_t$, and interact in a perturbative manner, the Standard Model Effective Field Theory (SMEFT) is a useful tool for describing physics phenomena at energy scales well below Λ .

$$\mathcal{L}_{\text{SMEFT}} = \mathcal{L}_{\text{SM}} + \frac{1}{\Lambda} \sum_k C_k^{(5)}(\mu) Q_k^{(5)} + \frac{1}{\Lambda^2} \sum_k C_k^{(6)}(\mu) Q_k^{(6)} + \mathcal{O}\left(\frac{1}{\Lambda^3}\right).$$

Flavor-changing processes that take place well below the electroweak scale are conveniently described in the Low-energy Effective Field Theory (LEFT) framework.

In new physics models where all the BSM particles have masses $m_1 \equiv \Lambda \leq m_2 \leq m_3 \dots m_n$, with $\Lambda \gg m_t$, and interact in a perturbative manner, the Standard Model Effective Field Theory (SMEFT) is a useful tool for describing physics phenomena at energy scales well below Λ .

$$\mathcal{L}_{\text{SMEFT}} = \mathcal{L}_{\text{SM}} + \frac{1}{\Lambda} \sum_k C_k^{(5)}(\mu) Q_k^{(5)} + \frac{1}{\Lambda^2} \sum_k C_k^{(6)}(\mu) Q_k^{(6)} + \mathcal{O}\left(\frac{1}{\Lambda^3}\right).$$

Flavor-changing processes that take place well below the electroweak scale are conveniently described in the Low-energy Effective Field Theory (LEFT) framework. LEFT is obtained from SMEFT through decoupling of the W -boson and all the heavier SM particles.

In new physics models where all the BSM particles have masses $m_1 \equiv \Lambda \leq m_2 \leq m_3 \dots m_n$, with $\Lambda \gg m_t$, and interact in a perturbative manner, the Standard Model Effective Field Theory (SMEFT) is a useful tool for describing physics phenomena at energy scales well below Λ .

$$\mathcal{L}_{\text{SMEFT}} = \mathcal{L}_{\text{SM}} + \frac{1}{\Lambda} \sum_k C_k^{(5)}(\mu) Q_k^{(5)} + \frac{1}{\Lambda^2} \sum_k C_k^{(6)}(\mu) Q_k^{(6)} + \mathcal{O}\left(\frac{1}{\Lambda^3}\right).$$

Flavor-changing processes that take place well below the electroweak scale are conveniently described in the Low-energy Effective Field Theory (LEFT) framework. LEFT is obtained from SMEFT through decoupling of the W -boson and all the heavier SM particles.

$$\begin{aligned} \mathcal{L}_{\text{LEFT}} = & \mathcal{L}_{\text{QCD} \times \text{QED}}(u, d, s, c, b, e, \mu, \tau) + \mathcal{L}_{\text{kin}}(\nu_e, \nu_\mu, \nu_\tau) \\ & + \frac{1}{M_W} \sum_k C_k^{(5)}(\mu) Q_k^{(5)} + \frac{1}{M_W^2} \sum_k C_k^{(6)}(\mu) Q_k^{(6)} + \mathcal{O}\left(\frac{1}{M_W^3}\right). \end{aligned}$$

In new physics models where all the BSM particles have masses $m_1 \equiv \Lambda \leq m_2 \leq m_3 \dots m_n$, with $\Lambda \gg m_t$, and interact in a perturbative manner, the Standard Model Effective Field Theory (SMEFT) is a useful tool for describing physics phenomena at energy scales well below Λ .

$$\mathcal{L}_{\text{SMEFT}} = \mathcal{L}_{\text{SM}} + \frac{1}{\Lambda} \sum_k C_k^{(5)}(\mu) Q_k^{(5)} + \frac{1}{\Lambda^2} \sum_k C_k^{(6)}(\mu) Q_k^{(6)} + \mathcal{O}\left(\frac{1}{\Lambda^3}\right).$$

Flavor-changing processes that take place well below the electroweak scale are conveniently described in the Low-energy Effective Field Theory (LEFT) framework. LEFT is obtained from SMEFT through decoupling of the W -boson and all the heavier SM particles.

$$\begin{aligned} \mathcal{L}_{\text{LEFT}} = & \mathcal{L}_{\text{QCD} \times \text{QED}}(u, d, s, c, b, e, \mu, \tau) + \mathcal{L}_{\text{kin}}(\nu_e, \nu_\mu, \nu_\tau) \\ & + \frac{1}{M_W} \sum_k C_k^{(5)}(\mu) Q_k^{(5)} + \frac{1}{M_W^2} \sum_k C_k^{(6)}(\mu) Q_k^{(6)} + \mathcal{O}\left(\frac{1}{M_W^3}\right). \end{aligned}$$

Generically: (Measured observable) = (SM contribution) + (BSM effect).

In new physics models where all the BSM particles have masses $m_1 \equiv \Lambda \leq m_2 \leq m_3 \dots m_n$, with $\Lambda \gg m_t$, and interact in a perturbative manner, the Standard Model Effective Field Theory (SMEFT) is a useful tool for describing physics phenomena at energy scales well below Λ .

$$\mathcal{L}_{\text{SMEFT}} = \mathcal{L}_{\text{SM}} + \frac{1}{\Lambda} \sum_k C_k^{(5)}(\mu) Q_k^{(5)} + \frac{1}{\Lambda^2} \sum_k C_k^{(6)}(\mu) Q_k^{(6)} + \mathcal{O}\left(\frac{1}{\Lambda^3}\right).$$

Flavor-changing processes that take place well below the electroweak scale are conveniently described in the Low-energy Effective Field Theory (LEFT) framework. LEFT is obtained from SMEFT through decoupling of the W -boson and all the heavier SM particles.

$$\begin{aligned} \mathcal{L}_{\text{LEFT}} = & \mathcal{L}_{\text{QCD} \times \text{QED}}(u, d, s, c, b, e, \mu, \tau) + \mathcal{L}_{\text{kin}}(\nu_e, \nu_\mu, \nu_\tau) \\ & + \frac{1}{M_W} \sum_k C_k^{(5)}(\mu) Q_k^{(5)} + \frac{1}{M_W^2} \sum_k C_k^{(6)}(\mu) Q_k^{(6)} + \mathcal{O}\left(\frac{1}{M_W^3}\right). \end{aligned}$$

Generically: (Measured observable) = $\underbrace{(\text{SM contribution})}_{\text{dominant}}$ + (BSM effect).

In new physics models where all the BSM particles have masses $m_1 \equiv \Lambda \leq m_2 \leq m_3 \dots m_n$, with $\Lambda \gg m_t$, and interact in a perturbative manner, the Standard Model Effective Field Theory (SMEFT) is a useful tool for describing physics phenomena at energy scales well below Λ .

$$\mathcal{L}_{\text{SMEFT}} = \mathcal{L}_{\text{SM}} + \frac{1}{\Lambda} \sum_k C_k^{(5)}(\mu) Q_k^{(5)} + \frac{1}{\Lambda^2} \sum_k C_k^{(6)}(\mu) Q_k^{(6)} + \mathcal{O}\left(\frac{1}{\Lambda^3}\right).$$

Flavor-changing processes that take place well below the electroweak scale are conveniently described in the Low-energy Effective Field Theory (LEFT) framework. LEFT is obtained from SMEFT through decoupling of the W -boson and all the heavier SM particles.

$$\begin{aligned} \mathcal{L}_{\text{LEFT}} = & \mathcal{L}_{\text{QCD} \times \text{QED}}(u, d, s, c, b, e, \mu, \tau) + \mathcal{L}_{\text{kin}}(\nu_e, \nu_\mu, \nu_\tau) \\ & + \frac{1}{M_W} \sum_k C_k^{(5)}(\mu) Q_k^{(5)} + \frac{1}{M_W^2} \sum_k C_k^{(6)}(\mu) Q_k^{(6)} + \mathcal{O}\left(\frac{1}{M_W^3}\right). \end{aligned}$$

$$\text{Generically:} \quad (\text{Measured observable}) = \underbrace{(\text{SM contribution})}_{\text{dominant}} + \underbrace{(\text{BSM effect})}_{\text{subdominant}}.$$

In new physics models where all the BSM particles have masses $m_1 \equiv \Lambda \leq m_2 \leq m_3 \dots m_n$, with $\Lambda \gg m_t$, and interact in a perturbative manner, the Standard Model Effective Field Theory (SMEFT) is a useful tool for describing physics phenomena at energy scales well below Λ .

$$\mathcal{L}_{\text{SMEFT}} = \mathcal{L}_{\text{SM}} + \frac{1}{\Lambda} \sum_k C_k^{(5)}(\mu) Q_k^{(5)} + \frac{1}{\Lambda^2} \sum_k C_k^{(6)}(\mu) Q_k^{(6)} + \mathcal{O}\left(\frac{1}{\Lambda^3}\right).$$

Flavor-changing processes that take place well below the electroweak scale are conveniently described in the Low-energy Effective Field Theory (LEFT) framework. LEFT is obtained from SMEFT through decoupling of the W -boson and all the heavier SM particles.

$$\begin{aligned} \mathcal{L}_{\text{LEFT}} = & \mathcal{L}_{\text{QCD} \times \text{QED}}(u, d, s, c, b, e, \mu, \tau) + \mathcal{L}_{\text{kin}}(\nu_e, \nu_\mu, \nu_\tau) \\ & + \frac{1}{M_W} \sum_k C_k^{(5)}(\mu) Q_k^{(5)} + \frac{1}{M_W^2} \sum_k C_k^{(6)}(\mu) Q_k^{(6)} + \mathcal{O}\left(\frac{1}{M_W^3}\right). \end{aligned}$$

Generically: (Measured observable) = $\underbrace{(\text{SM contribution})}_{\text{dominant}}$ + $\underbrace{(\text{BSM effect})}_{\text{subdominant}}$.

\Rightarrow TH precision necessary

In new physics models where all the BSM particles have masses $m_1 \equiv \Lambda \leq m_2 \leq m_3 \dots m_n$, with $\Lambda \gg m_t$, and interact in a perturbative manner, the Standard Model Effective Field Theory (SMEFT) is a useful tool for describing physics phenomena at energy scales well below Λ .

$$\mathcal{L}_{\text{SMEFT}} = \mathcal{L}_{\text{SM}} + \frac{1}{\Lambda} \sum_k C_k^{(5)}(\mu) Q_k^{(5)} + \frac{1}{\Lambda^2} \sum_k C_k^{(6)}(\mu) Q_k^{(6)} + \mathcal{O}\left(\frac{1}{\Lambda^3}\right).$$

Flavor-changing processes that take place well below the electroweak scale are conveniently described in the Low-energy Effective Field Theory (LEFT) framework. LEFT is obtained from SMEFT through decoupling of the W -boson and all the heavier SM particles.

$$\begin{aligned} \mathcal{L}_{\text{LEFT}} = & \mathcal{L}_{\text{QCD} \times \text{QED}}(u, d, s, c, b, e, \mu, \tau) + \mathcal{L}_{\text{kin}}(\nu_e, \nu_\mu, \nu_\tau) \\ & + \frac{1}{M_W} \sum_k C_k^{(5)}(\mu) Q_k^{(5)} + \frac{1}{M_W^2} \sum_k C_k^{(6)}(\mu) Q_k^{(6)} + \mathcal{O}\left(\frac{1}{M_W^3}\right). \end{aligned}$$

Generically: (Measured observable) = $\underbrace{(\text{SM contribution})}_{\substack{\text{dominant} \\ \Rightarrow \text{TH precision necessary}}} + \underbrace{(\text{BSM effect})}_{\substack{\text{subdominant} \\ \text{rough calculations sufficient}}}$.

In new physics models where all the BSM particles have masses $m_1 \equiv \Lambda \leq m_2 \leq m_3 \dots m_n$, with $\Lambda \gg m_t$, and interact in a perturbative manner, the Standard Model Effective Field Theory (SMEFT) is a useful tool for describing physics phenomena at energy scales well below Λ .

$$\mathcal{L}_{\text{SMEFT}} = \mathcal{L}_{\text{SM}} + \frac{1}{\Lambda} \sum_k C_k^{(5)}(\mu) Q_k^{(5)} + \frac{1}{\Lambda^2} \sum_k C_k^{(6)}(\mu) Q_k^{(6)} + \mathcal{O}\left(\frac{1}{\Lambda^3}\right).$$

Flavor-changing processes that take place well below the electroweak scale are conveniently described in the Low-energy Effective Field Theory (LEFT) framework. LEFT is obtained from SMEFT through decoupling of the W -boson and all the heavier SM particles.

$$\begin{aligned} \mathcal{L}_{\text{LEFT}} = & \mathcal{L}_{\text{QCD} \times \text{QED}}(u, d, s, c, b, e, \mu, \tau) + \mathcal{L}_{\text{kin}}(\nu_e, \nu_\mu, \nu_\tau) \\ & + \frac{1}{M_W} \sum_k C_k^{(5)}(\mu) Q_k^{(5)} + \frac{1}{M_W^2} \sum_k C_k^{(6)}(\mu) Q_k^{(6)} + \mathcal{O}\left(\frac{1}{M_W^3}\right). \end{aligned}$$

Generically:	(Measured observable)	=	(SM contribution)	+	(BSM effect).
			<u>dominant</u>		<u>subdominant</u>
			\Rightarrow TH precision necessary		rough calculations sufficient

Exceptions: neutrino masses, dark matter, ...

In new physics models where all the BSM particles have masses $m_1 \equiv \Lambda \leq m_2 \leq m_3 \dots m_n$, with $\Lambda \gg m_t$, and interact in a perturbative manner, the Standard Model Effective Field Theory (SMEFT) is a useful tool for describing physics phenomena at energy scales well below Λ .

$$\mathcal{L}_{\text{SMEFT}} = \mathcal{L}_{\text{SM}} + \frac{1}{\Lambda} \sum_k C_k^{(5)}(\mu) Q_k^{(5)} + \frac{1}{\Lambda^2} \sum_k C_k^{(6)}(\mu) Q_k^{(6)} + \mathcal{O}\left(\frac{1}{\Lambda^3}\right).$$

Flavor-changing processes that take place well below the electroweak scale are conveniently described in the Low-energy Effective Field Theory (LEFT) framework. LEFT is obtained from SMEFT through decoupling of the W -boson and all the heavier SM particles.

$$\begin{aligned} \mathcal{L}_{\text{LEFT}} = & \mathcal{L}_{\text{QCD} \times \text{QED}}(u, d, s, c, b, e, \mu, \tau) + \mathcal{L}_{\text{kin}}(\nu_e, \nu_\mu, \nu_\tau) \\ & + \frac{1}{M_W} \sum_k C_k^{(5)}(\mu) Q_k^{(5)} + \frac{1}{M_W^2} \sum_k C_k^{(6)}(\mu) Q_k^{(6)} + \mathcal{O}\left(\frac{1}{M_W^3}\right). \end{aligned}$$

$$\begin{array}{llll} \text{Generically:} & (\text{Measured observable}) & = & \underbrace{(\text{SM contribution})}_{\substack{\text{dominant} \\ \Rightarrow \text{TH precision necessary}}} + \underbrace{(\text{BSM effect})}_{\substack{\text{subdominant} \\ \text{rough calculations sufficient}}} \end{array}$$

Exceptions: neutrino masses, dark matter, ...

In collider physics?

In new physics models where all the BSM particles have masses $m_1 \equiv \Lambda \leq m_2 \leq m_3 \dots m_n$, with $\Lambda \gg m_t$, and interact in a perturbative manner, the Standard Model Effective Field Theory (SMEFT) is a useful tool for describing physics phenomena at energy scales well below Λ .

$$\mathcal{L}_{\text{SMEFT}} = \mathcal{L}_{\text{SM}} + \frac{1}{\Lambda} \sum_k C_k^{(5)}(\mu) Q_k^{(5)} + \frac{1}{\Lambda^2} \sum_k C_k^{(6)}(\mu) Q_k^{(6)} + \mathcal{O}\left(\frac{1}{\Lambda^3}\right).$$

Flavor-changing processes that take place well below the electroweak scale are conveniently described in the Low-energy Effective Field Theory (LEFT) framework. LEFT is obtained from SMEFT through decoupling of the W -boson and all the heavier SM particles.

$$\begin{aligned} \mathcal{L}_{\text{LEFT}} = & \mathcal{L}_{\text{QCD} \times \text{QED}}(u, d, s, c, b, e, \mu, \tau) + \mathcal{L}_{\text{kin}}(\nu_e, \nu_\mu, \nu_\tau) \\ & + \frac{1}{M_W} \sum_k C_k^{(5)}(\mu) Q_k^{(5)} + \frac{1}{M_W^2} \sum_k C_k^{(6)}(\mu) Q_k^{(6)} + \mathcal{O}\left(\frac{1}{M_W^3}\right). \end{aligned}$$

Generically:	(Measured observable)	=	$\underbrace{(\text{SM contribution})}_{\text{dominant}}$	+	$\underbrace{(\text{BSM effect})}_{\text{subdominant}}$
			\Rightarrow TH precision necessary		rough calculations sufficient

Exceptions: neutrino masses, dark matter, ...

In collider physics? $b \rightarrow s \ell^+ \ell^-$?

In new physics models where all the BSM particles have masses $m_1 \equiv \Lambda \leq m_2 \leq m_3 \dots m_n$, with $\Lambda \gg m_t$, and interact in a perturbative manner, the Standard Model Effective Field Theory (SMEFT) is a useful tool for describing physics phenomena at energy scales well below Λ .

$$\mathcal{L}_{\text{SMEFT}} = \mathcal{L}_{\text{SM}} + \frac{1}{\Lambda} \sum_k C_k^{(5)}(\mu) Q_k^{(5)} + \frac{1}{\Lambda^2} \sum_k C_k^{(6)}(\mu) Q_k^{(6)} + \mathcal{O}\left(\frac{1}{\Lambda^3}\right).$$

Flavor-changing processes that take place well below the electroweak scale are conveniently described in the Low-energy Effective Field Theory (LEFT) framework. LEFT is obtained from SMEFT through decoupling of the W -boson and all the heavier SM particles.

$$\begin{aligned} \mathcal{L}_{\text{LEFT}} = & \mathcal{L}_{\text{QCD} \times \text{QED}}(u, d, s, c, b, e, \mu, \tau) + \mathcal{L}_{\text{kin}}(\nu_e, \nu_\mu, \nu_\tau) \\ & + \frac{1}{M_W} \sum_k C_k^{(5)}(\mu) Q_k^{(5)} + \frac{1}{M_W^2} \sum_k C_k^{(6)}(\mu) Q_k^{(6)} + \mathcal{O}\left(\frac{1}{M_W^3}\right). \end{aligned}$$

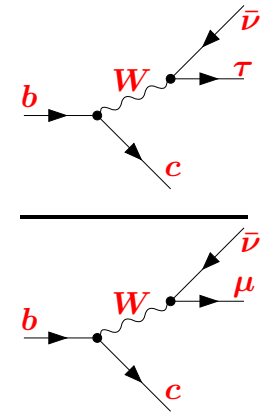
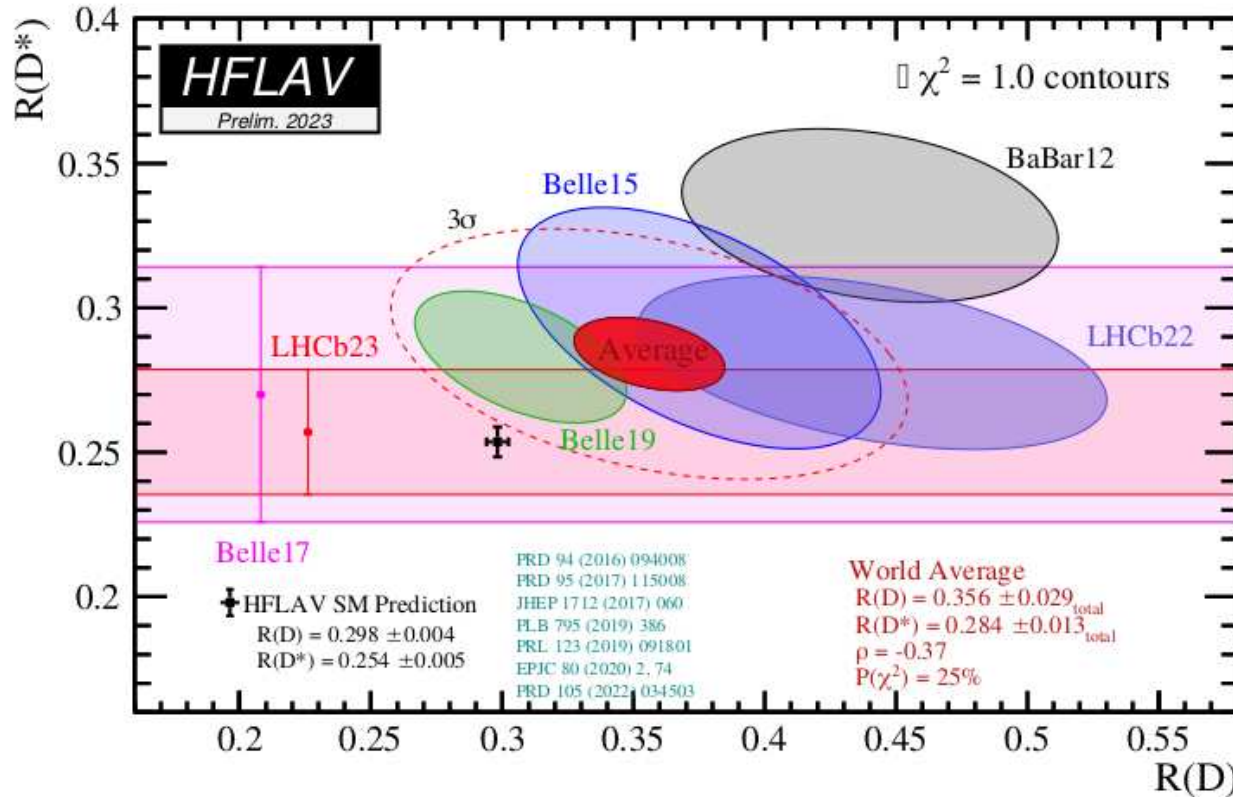
$$\begin{array}{llll} \text{Generically:} & (\text{Measured observable}) & = & \underbrace{(\text{SM contribution})}_{\substack{\text{dominant} \\ \Rightarrow \text{TH precision necessary}}} + \underbrace{(\text{BSM effect})}_{\substack{\text{subdominant} \\ \text{rough calculations sufficient}}} \end{array}$$

Exceptions: neutrino masses, dark matter, ...

In collider physics? $b \rightarrow s \ell^+ \ell^-$? $R_{D^{(*)}}$?

Ratios of exclusive semileptonic branching ratios

$$R(D^{(*)}) = \mathcal{B}(B \rightarrow D^{(*)}\tau\bar{\nu})/\mathcal{B}(B \rightarrow D^{(*)}\mu\bar{\nu}) \quad \text{after March 21st, 2023:}$$



A $\sim 3\sigma$ deviation from the SM remains.

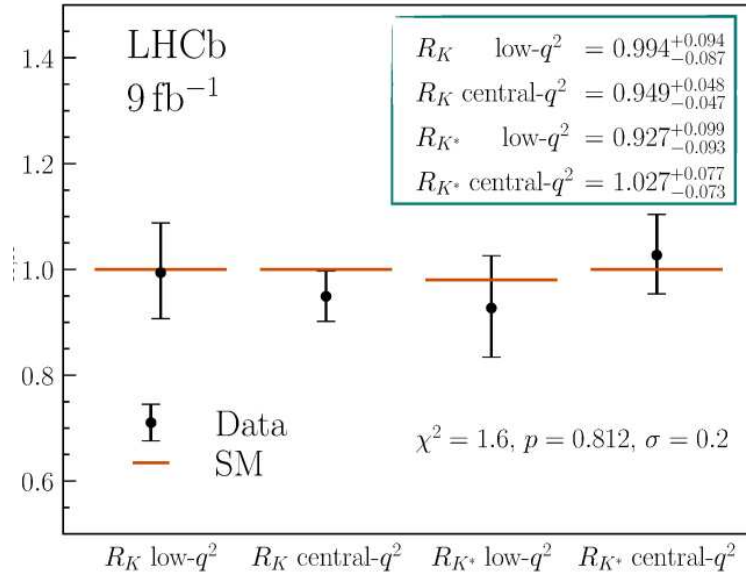
Large BSM effect or an experimental issue?

Deviations from SM predictions in $b \rightarrow s\ell^+\ell^-$ transitions?

Recent LHCb measurement of

$$R_{K^{(*)}} = \frac{\mathcal{B}(B \rightarrow K^{(*)} \mu^+ \mu^-)}{\mathcal{B}(B \rightarrow K^{(*)} e^+ e^-)}$$

[arXiv:2212.09153]



low q^2 : [0.1, 1, 1] GeV²

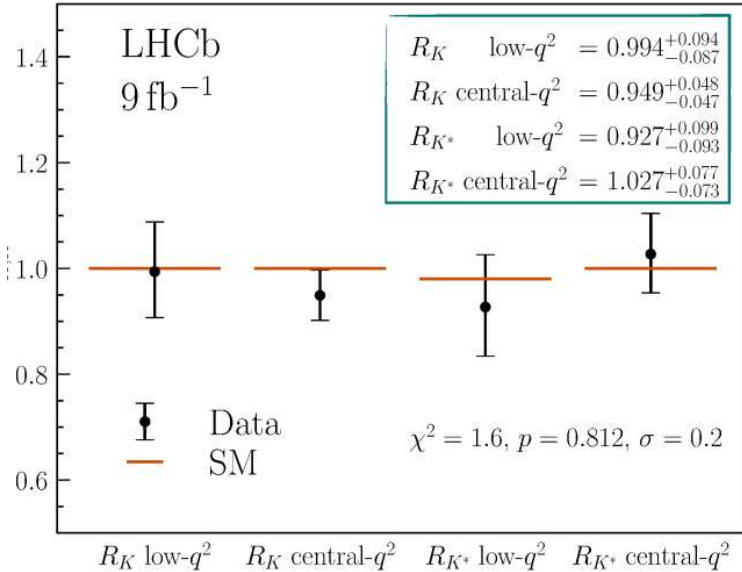
central q^2 : [1.1, 6.0] GeV²

Deviations from SM predictions in $b \rightarrow s\ell^+\ell^-$ transitions?

Recent LHCb measurement of

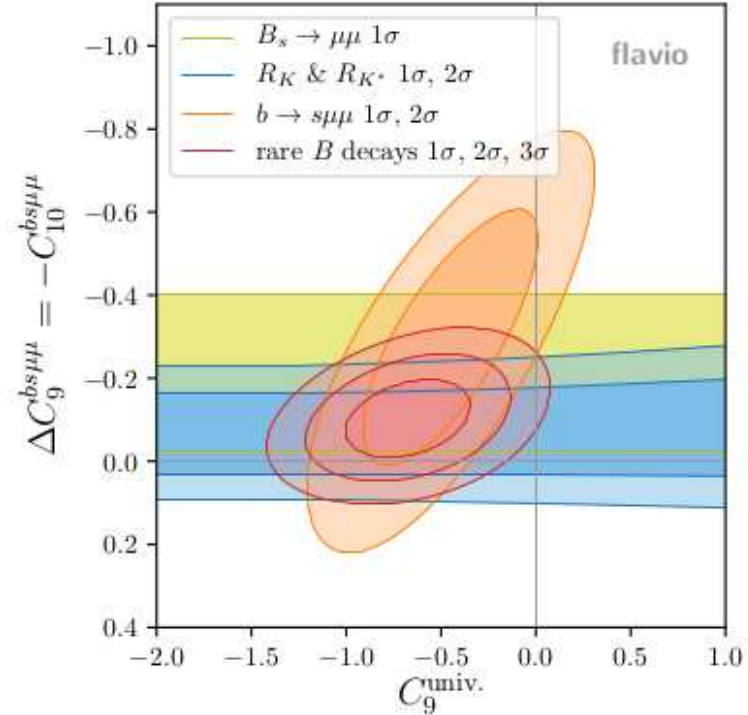
$$R_{K^{(*)}} = \frac{\mathcal{B}(B \rightarrow K^{(*)} \mu^+ \mu^-)}{\mathcal{B}(B \rightarrow K^{(*)} e^+ e^-)}$$

[arXiv:2212.09153]



low q^2 : [0.1, 1, 1] GeV²
 central q^2 : [1.1, 6.0] GeV²

Sample constraints on the $bsll$ operator Wilson coefficients from arXiv:2212.10497 by A. Greljo, J. Salko, A. Smolkovič, P. Stangl:

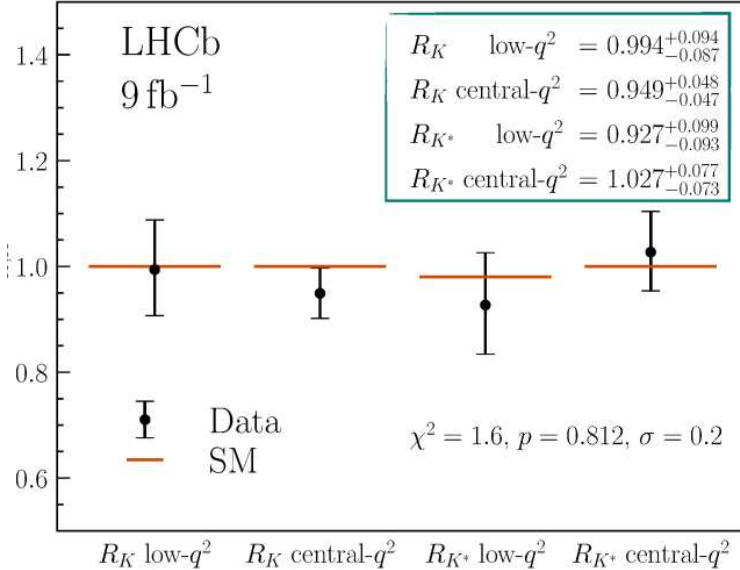


Deviations from SM predictions in $b \rightarrow s \ell^+ \ell^-$ transitions?

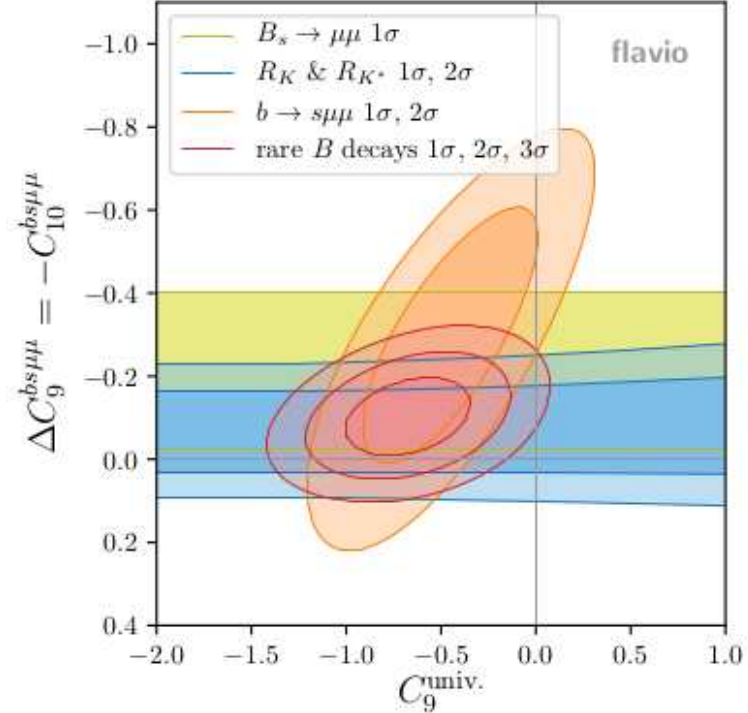
Recent LHCb measurement of

$$R_{K^{(*)}} = \frac{\mathcal{B}(B \rightarrow K^{(*)} \mu^+ \mu^-)}{\mathcal{B}(B \rightarrow K^{(*)} e^+ e^-)}$$

[arXiv:2212.09153]



Sample constraints on the $bsll$ operator Wilson coefficients from arXiv:2212.10497 by A. Greljo, J. Salko, A. Smolkovič, P. Stangl:



Possible charm-loop effects that could mimic a deviation in C_9^{univ} :

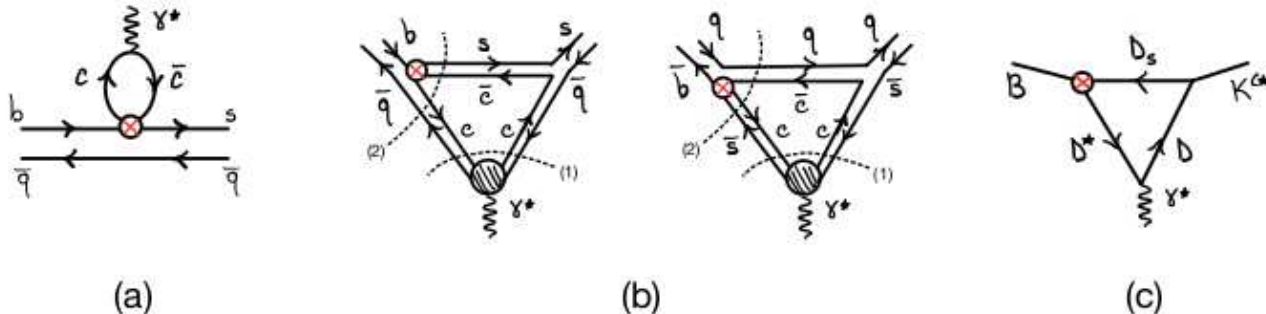
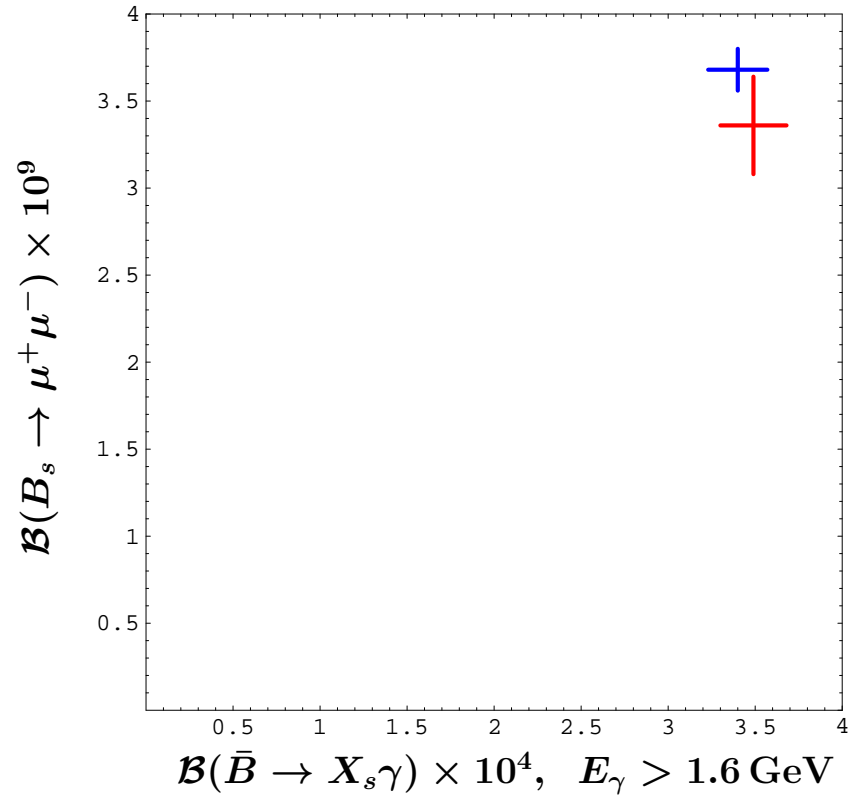
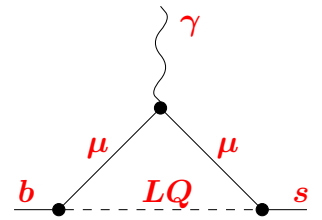
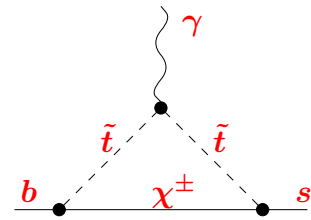
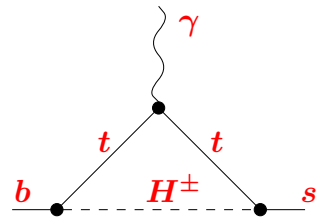
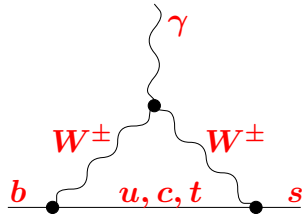
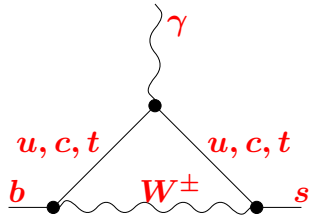
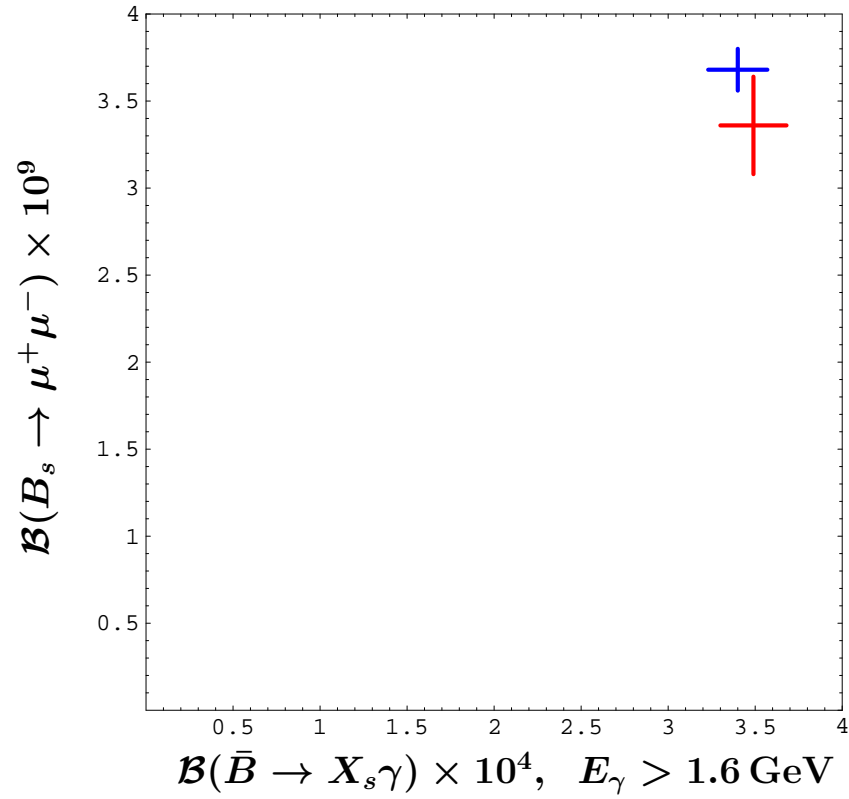


Fig. 1 from arXiv:2212.10516 by M. Ciuchini, M. Fedele, E. Franco, A. Paul, L. Silvestrini and M. Valli.

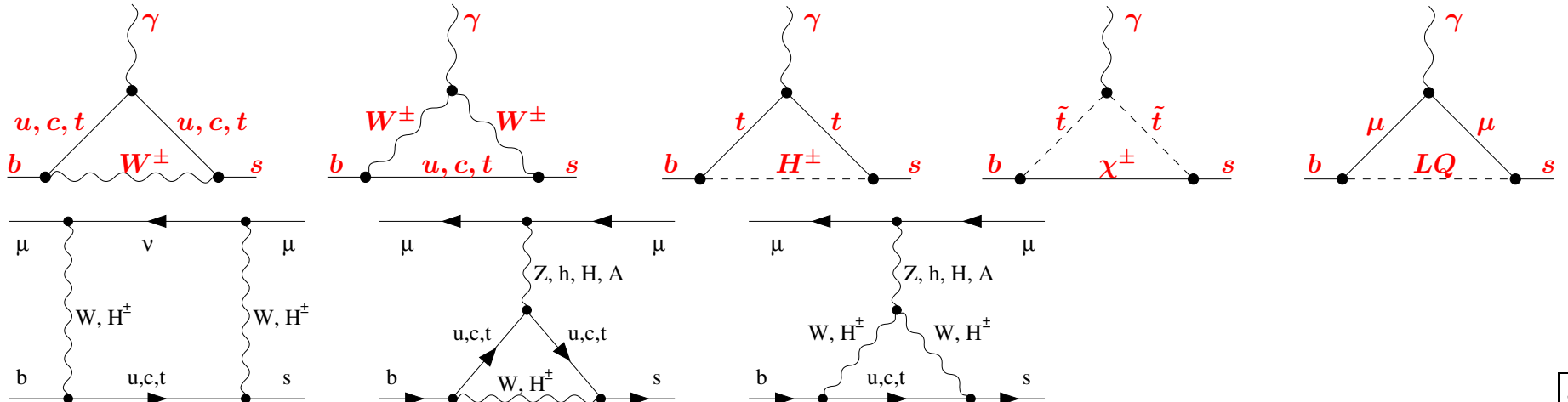
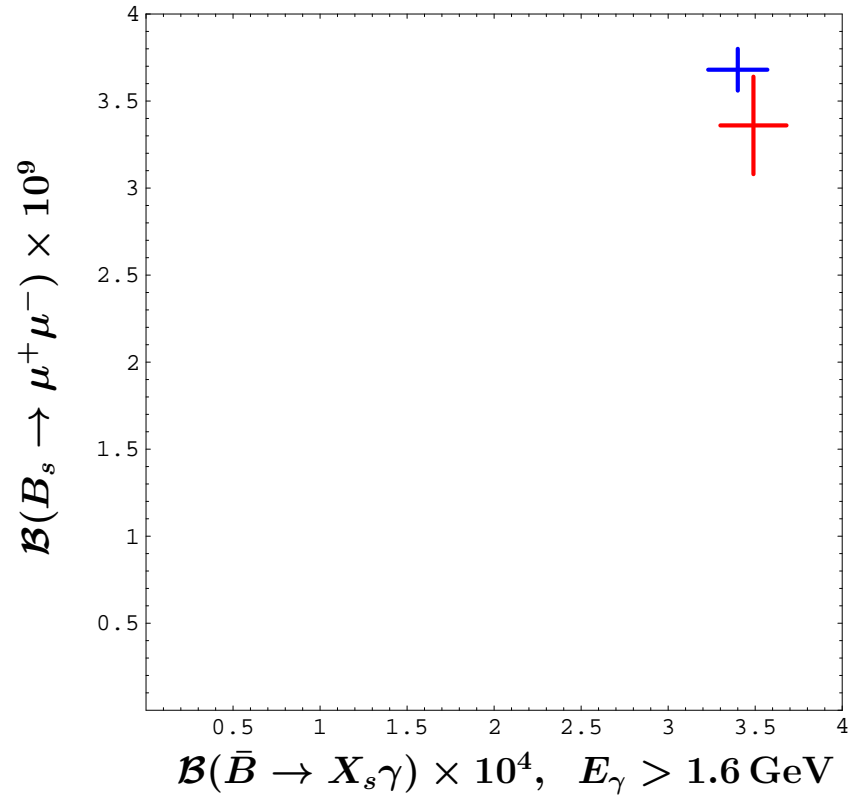
SM predictions vs. measurements for $\mathcal{B}(\bar{B} \rightarrow X_s \gamma)$ and $\mathcal{B}(B_s \rightarrow \mu^+ \mu^-)$



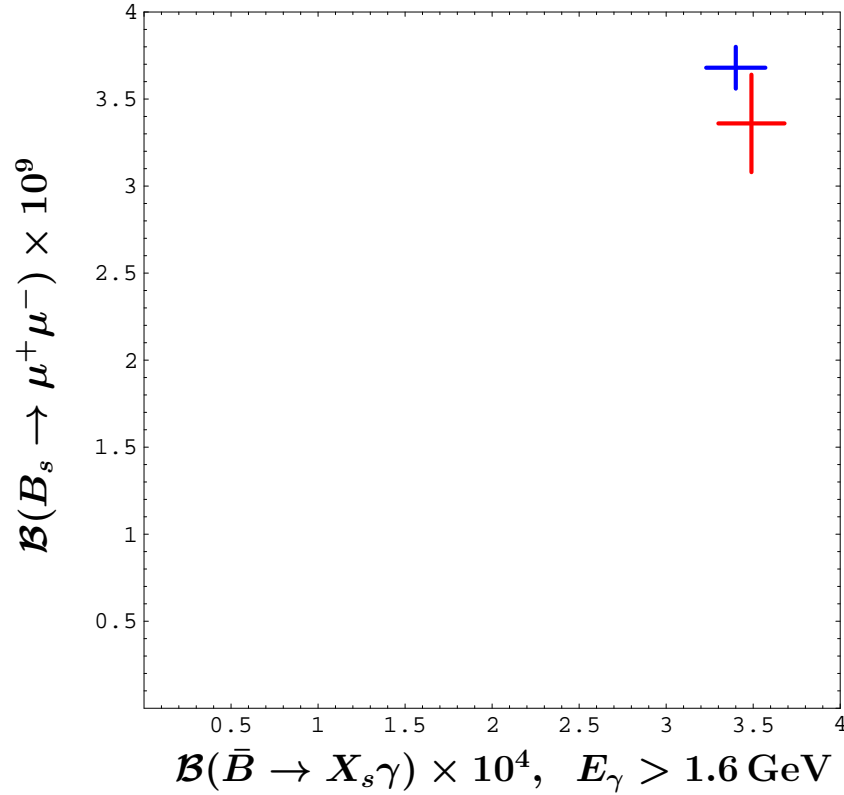
SM predictions vs. measurements for $\mathcal{B}(\bar{B} \rightarrow X_s \gamma)$ and $\mathcal{B}(B_s \rightarrow \mu^+ \mu^-)$



SM predictions vs. measurements for $\mathcal{B}(\bar{B} \rightarrow X_s \gamma)$ and $\mathcal{B}(B_s \rightarrow \mu^+ \mu^-)$

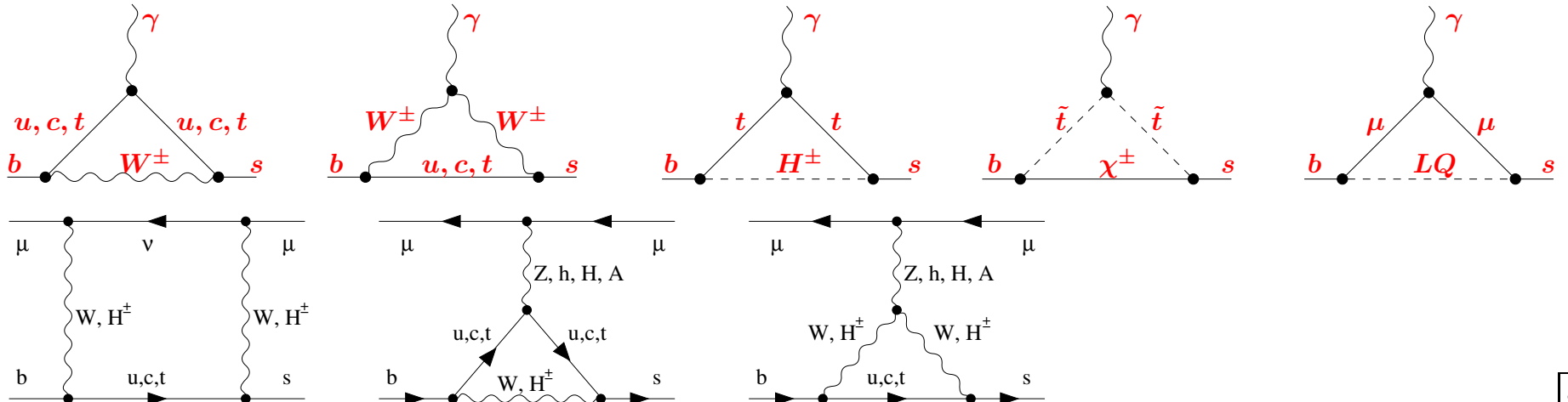


SM predictions vs. measurements for $\mathcal{B}(\bar{B} \rightarrow X_s \gamma)$ and $\mathcal{B}(B_s \rightarrow \mu^+ \mu^-)$

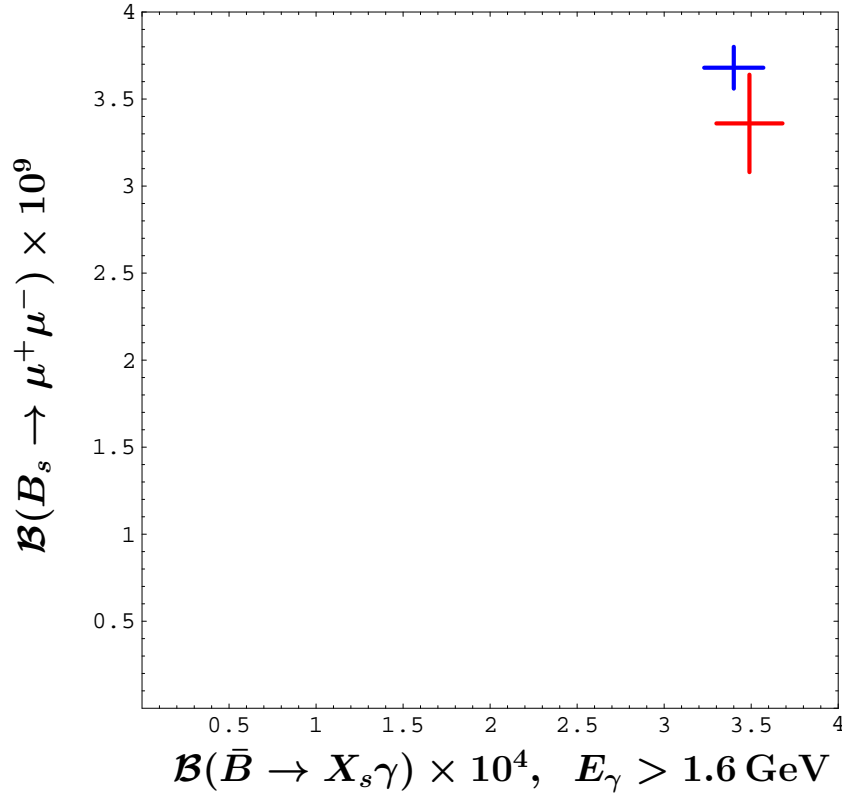


$$\mathcal{B}(\bar{B} \rightarrow X_s \gamma)_{E_\gamma > 1.6}^{\text{exp}} \times 10^4 = 3.49 \pm 0.19 \quad (\pm 5.4\%)$$

CLEO, BaBar and Belle measurements combined
by PDG [2022] and HFLAV [arXiv:2206.07501].



SM predictions vs. measurements for $\mathcal{B}(\bar{B} \rightarrow X_s \gamma)$ and $\mathcal{B}(B_s \rightarrow \mu^+ \mu^-)$

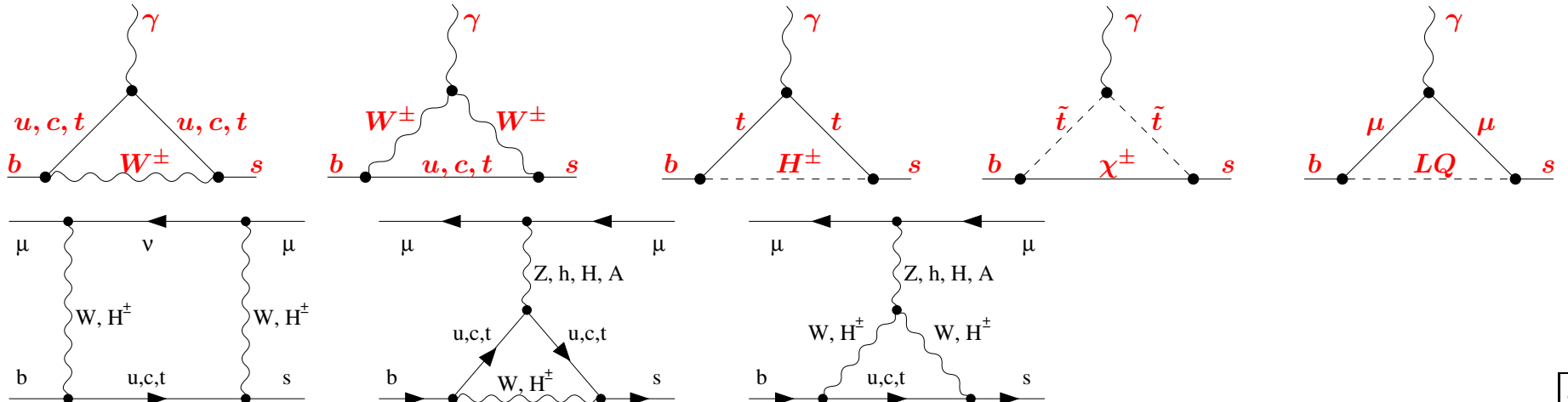


$$\mathcal{B}(\bar{B} \rightarrow X_s \gamma)_{E_\gamma > 1.6}^{\text{exp}} \times 10^4 = 3.49 \pm 0.19 \quad (\pm 5.4\%)$$

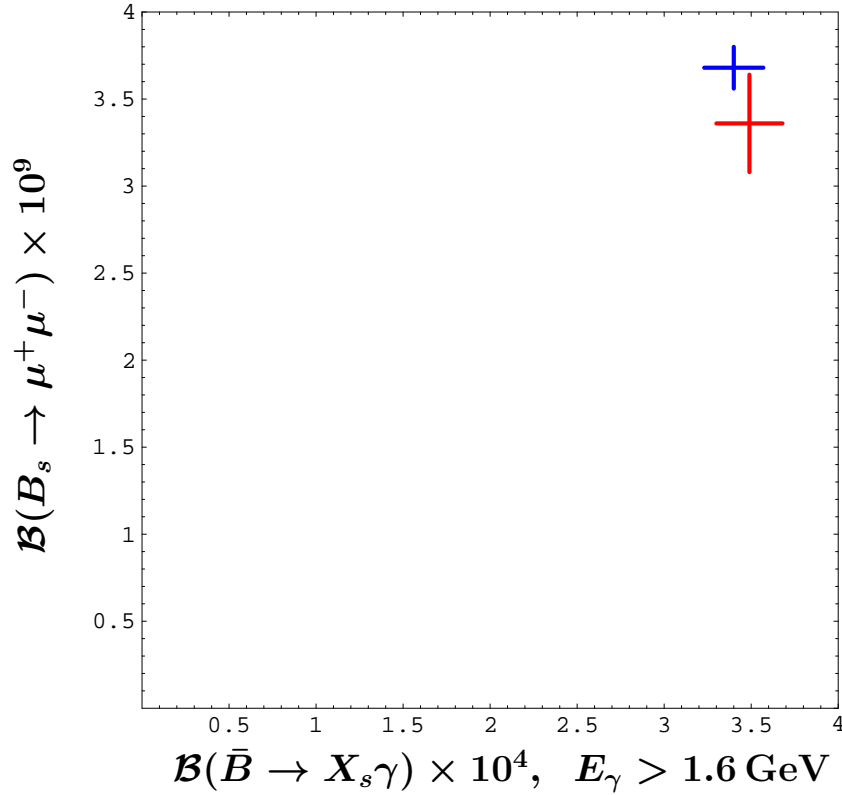
CLEO, BaBar and Belle measurements combined
by PDG [2022] and HFLAV [arXiv:2206.07501].

$$\mathcal{B}(\bar{B} \rightarrow X_s \gamma)_{E_\gamma > 1.6}^{\text{SM}} \times 10^4 = 3.40 \pm 0.17 \quad (\pm 5.0\%)$$

arXiv:2002.01548 by MM, A. Rehman, M. Steinhauser.



SM predictions vs. measurements for $\mathcal{B}(\bar{B} \rightarrow X_s \gamma)$ and $\mathcal{B}(B_s \rightarrow \mu^+ \mu^-)$



$$\mathcal{B}(\bar{B} \rightarrow X_s \gamma)_{E_\gamma > 1.6}^{\text{exp}} \times 10^4 = 3.49 \pm 0.19 \quad (\pm 5.4\%)$$

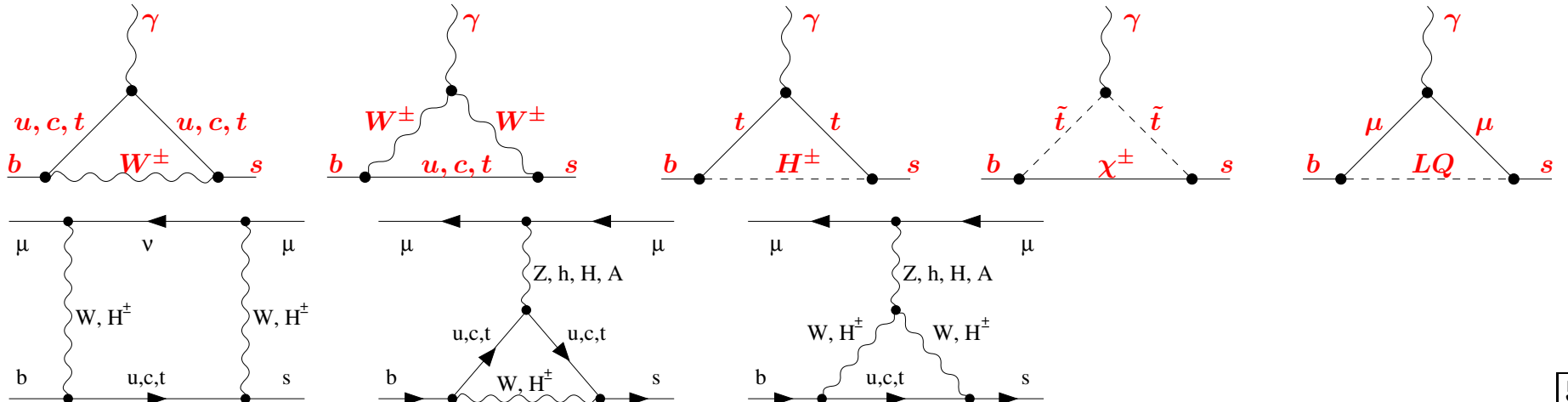
CLEO, BaBar and Belle measurements combined by PDG [2022] and HFLAV [arXiv:2206.07501].

$$\mathcal{B}(\bar{B} \rightarrow X_s \gamma)_{E_\gamma > 1.6}^{\text{SM}} \times 10^4 = 3.40 \pm 0.17 \quad (\pm 5.0\%)$$

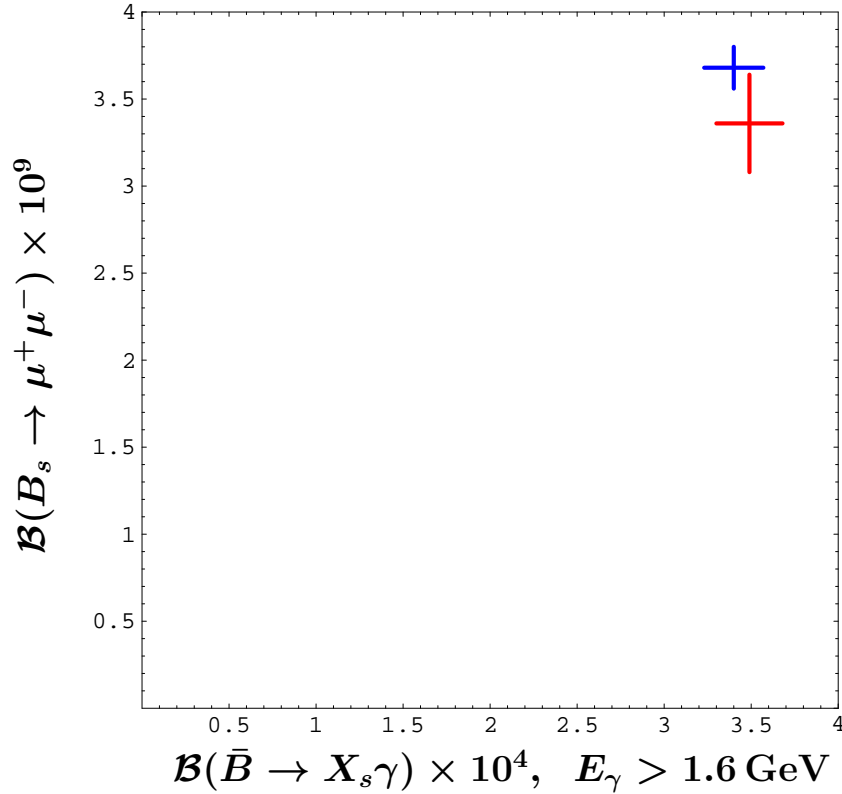
arXiv:2002.01548 by MM, A. Rehman, M. Steinhauser.

$$\mathcal{B}(B_s \rightarrow \mu^+ \mu^-)^{\text{exp}} \times 10^9 = 3.36 \pm 0.28 \quad (\pm 8.3\%)$$

LHCb'21, CMS'22 and ATLAS'18 measurements combined in arXiv:2212.10497 by A. Greljo, J. Salko, A. Smolkovič, P. Stangl.



SM predictions vs. measurements for $\mathcal{B}(\bar{B} \rightarrow X_s \gamma)$ and $\mathcal{B}(B_s \rightarrow \mu^+ \mu^-)$



$$\mathcal{B}(\bar{B} \rightarrow X_s \gamma)_{E_\gamma > 1.6}^{\text{exp}} \times 10^4 = 3.49 \pm 0.19 \quad (\pm 5.4\%)$$

CLEO, BaBar and Belle measurements combined by PDG [2022] and HFLAV [arXiv:2206.07501].

$$\mathcal{B}(\bar{B} \rightarrow X_s \gamma)_{E_\gamma > 1.6}^{\text{SM}} \times 10^4 = 3.40 \pm 0.17 \quad (\pm 5.0\%)$$

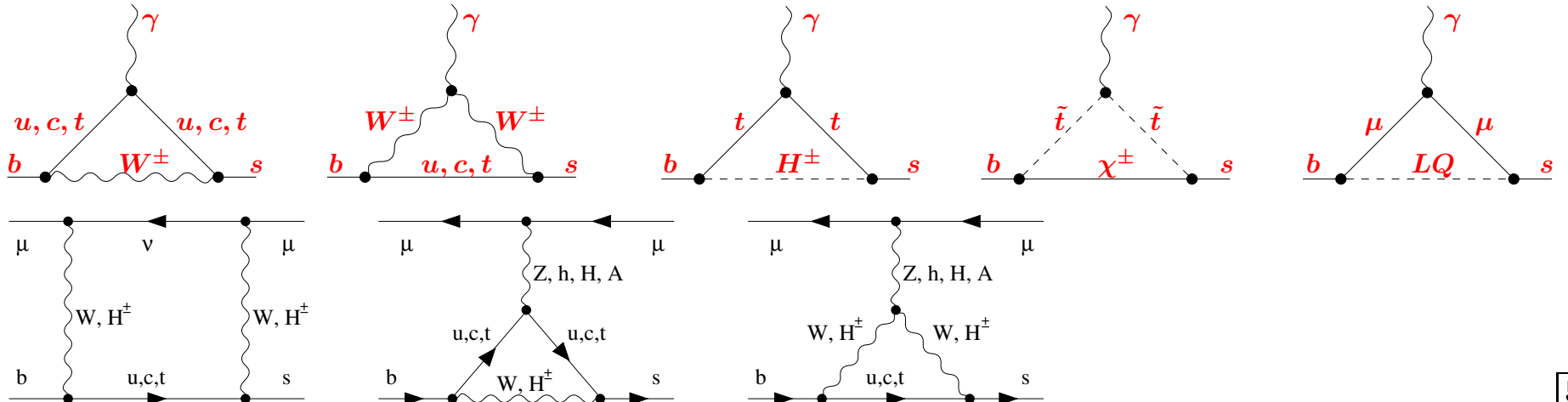
arXiv:2002.01548 by MM, A. Rehman, M. Steinhauser.

$$\mathcal{B}(B_s \rightarrow \mu^+ \mu^-)^{\text{exp}} \times 10^9 = 3.36 \pm 0.28 \quad (\pm 8.3\%)$$

LHCb'21, CMS'22 and ATLAS'18 measurements combined in arXiv:2212.10497 by A. Greljo, J. Salko, A. Smolkovič, P. Stangl.

$$\mathcal{B}(B_s \rightarrow \mu^+ \mu^-)^{\text{SM}} \times 10^9 = 3.68 \pm 0.12 \quad (\pm 3.2\%)$$

arXiv:1311.0903 by C. Bobeth, M. Gorbahn, T. Hermann, MM, E. Stamou, M. Steinhauser **with parameter updates (next slides)** and -0.5% QED correction from arXiv:1907.07011 by M. Beneke, C. Bobeth and R. Szafron.



Input parameter update for $B_{s,d} \rightarrow \ell^+ \ell^-$

	arXiv:1311.0903	this talk	source
M_t [GeV]	173.1(9)	172.69(30)	PDG'23, https://pdglive.lbl.gov
$\alpha_s(M_Z)$	0.1184(7)	0.1179(9)	PDG'22, https://pdg.lbl.gov
f_{B_s} [GeV]	0.2277(45)	0.2303(13)	FLAG'23, http://flag.unibe.ch
f_{B_d} [GeV]	0.1905(42)	0.1900(13)	FLAG'23, http://flag.unibe.ch
$ V_{cb} \times 10^3$	42.40(90)	42.16(50)	inclusive, arXiv:2107.00604
$ V_{tb}^* V_{ts} / V_{cb} $	0.9800(10)	0.9818(5)	derived from <i>UTfit</i> , arXiv:2212.03894
$ V_{tb}^* V_{td} \times 10^2$	0.88(3)	0.859(11)	<i>UTfit</i> , arXiv:2212.03894
τ_H^s [ps]	1.615(21)	1.624(9)	HFLAV'23, https://hflav.web.cern.ch
τ_H^d [ps]	1.519(7)	1.519(4)	HFLAV'23, https://hflav.web.cern.ch
$\overline{\mathcal{B}}_{s\mu} \times 10^9$	3.65(23)	3.68(12)	
$\overline{\mathcal{B}}_{d\mu} \times 10^{10}$	1.06(9)	0.99(4)	

Sources of uncertainties	f_{B_q}	CKM	τ_H^q	M_t	α_s	other parametric	non- parametric	Σ
$\overline{\mathcal{B}}_{s\ell}$	1.1%	2.4%	0.6%	0.5%	0.2%	< 0.1%	1.5%	3.2%
$\overline{\mathcal{B}}_{d\ell}$	1.4%	2.6%	0.3%	0.5%	0.2%	< 0.1%	1.5%	3.6%

SM predictions for all the branching ratios $\overline{\mathcal{B}}_{q\ell} \equiv \overline{\mathcal{B}}(B_q^0 \rightarrow \ell^+ \ell^-)$ including 2-loop electroweak and 3-loop QCD matching at $\mu_0 \sim m_t$
 [C. Bobeth, M. Gorbahn, T. Hermann, MM, E. Stamou, M. Steinhauser, arXiv:1311.0903]

$$\begin{aligned}\overline{\mathcal{B}}_{se} \times 10^{14} &= \eta_{\text{QED}} (8.54 \pm 0.13) R_{t\alpha} R_s, \\ \overline{\mathcal{B}}_{s\mu} \times 10^9 &= \eta_{\text{QED}} (3.65 \pm 0.06) R_{t\alpha} R_s, \\ \overline{\mathcal{B}}_{s\tau} \times 10^7 &= \eta_{\text{QED}} (7.73 \pm 0.12) R_{t\alpha} R_s, \\ \overline{\mathcal{B}}_{de} \times 10^{15} &= \eta_{\text{QED}} (2.48 \pm 0.04) R_{t\alpha} R_d, \\ \overline{\mathcal{B}}_{d\mu} \times 10^{10} &= \eta_{\text{QED}} (1.06 \pm 0.02) R_{t\alpha} R_d, \\ \overline{\mathcal{B}}_{d\tau} \times 10^8 &= \eta_{\text{QED}} (2.22 \pm 0.04) R_{t\alpha} R_d,\end{aligned}$$

where

$$\begin{aligned}R_{t\alpha} &= \left(\frac{M_t}{173.1 \text{ GeV}} \right)^{3.06} \left(\frac{\alpha_s(M_Z)}{0.1184} \right)^{-0.18}, \\ R_s &= \left(\frac{f_{B_s} [\text{MeV}]}{227.7} \right)^2 \left(\frac{|V_{cb}|}{0.0424} \right)^2 \left(\frac{|V_{tb}^* V_{ts} / V_{cb}|}{0.980} \right)^2 \frac{\tau_H^s [\text{ps}]}{1.615}, \\ R_d &= \left(\frac{f_{B_d} [\text{MeV}]}{190.5} \right)^2 \left(\frac{|V_{tb}^* V_{td}|}{0.0088} \right)^2 \frac{\tau_d^{\text{av}} [\text{ps}]}{1.519}.\end{aligned}$$

Enhanced QED effects in $B_q \rightarrow \ell^+ \ell^-$

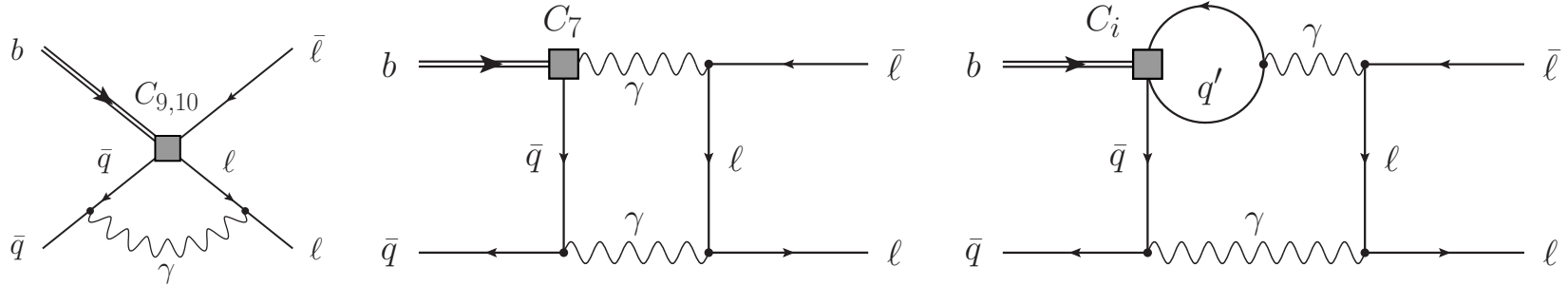
The leading contribution to the decay rate is suppressed by $\frac{m_\ell^2}{M_{B_q}^2}$.

.

Enhanced QED effects in $B_q \rightarrow \ell^+ \ell^-$

The leading contribution to the decay rate is suppressed by $\frac{m_\ell^2}{M_{B_q}^2}$.

As observed by M. Beneke, C. Bobeth and R. Szafron in arXiv:1708.09152,
some of the QED corrections receive suppression by $\frac{m_\ell^2}{\Lambda M_{B_q}}$ only:



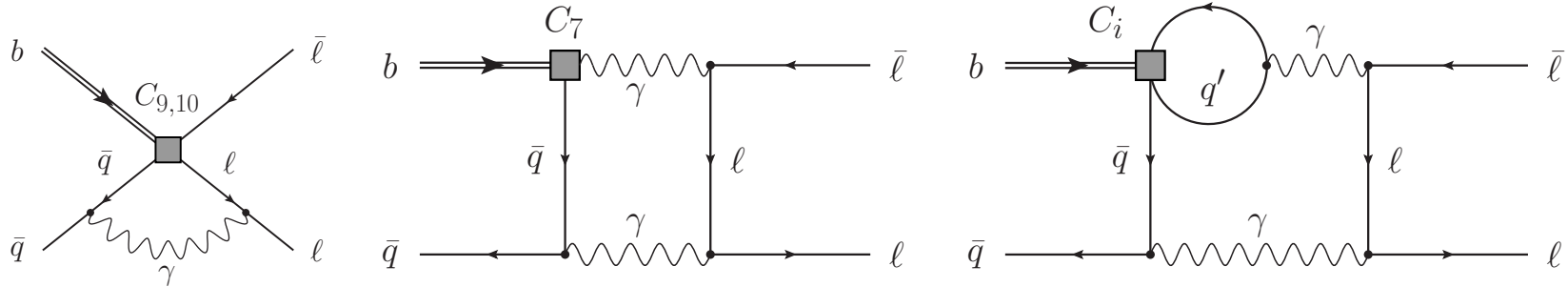
See also the lecture by RS at the Paris-2019 workshop:

<https://indico.in2p3.fr/event/18845/sessions/12137/attachments/54326/71064/Szafron.pdf>

Enhanced QED effects in $B_q \rightarrow \ell^+ \ell^-$

The leading contribution to the decay rate is suppressed by $\frac{m_\ell^2}{M_{B_q}^2}$.

As observed by M. Beneke, C. Bobeth and R. Szafron in arXiv:1708.09152,
some of the QED corrections receive suppression by $\frac{m_\ell^2}{\Lambda M_{B_q}}$ only:



See also the lecture by RS at the Paris-2019 workshop:

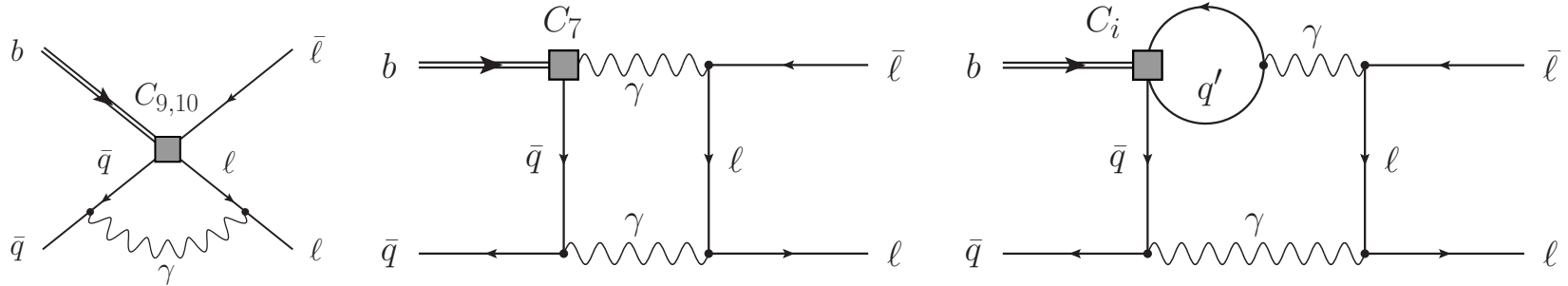
<https://indico.in2p3.fr/event/18845/sessions/12137/attachments/54326/71064/Szafron.pdf>

Consequently, the relative QED correction scales like $\frac{\alpha_{em}}{\pi} \frac{M_{B_q}}{\Lambda}$.

Enhanced QED effects in $B_q \rightarrow \ell^+ \ell^-$

The leading contribution to the decay rate is suppressed by $\frac{m_\ell^2}{M_{B_q}^2}$.

As observed by M. Beneke, C. Bobeth and R. Szafron in arXiv:1708.09152, some of the QED corrections receive suppression by $\frac{m_\ell^2}{\Lambda M_{B_q}}$ only:



See also the lecture by RS at the Paris-2019 workshop:

<https://indico.in2p3.fr/event/18845/sessions/12137/attachments/54326/71064/Szafron.pdf>

Consequently, the relative QED correction scales like $\frac{\alpha_{em}}{\pi} \frac{M_{B_q}}{\Lambda}$.

Their explicit calculation in arXiv:1908.07011 implies that the previous results for all the $B_q \rightarrow \ell^+ \ell^-$ branching ratios need to be multiplied by

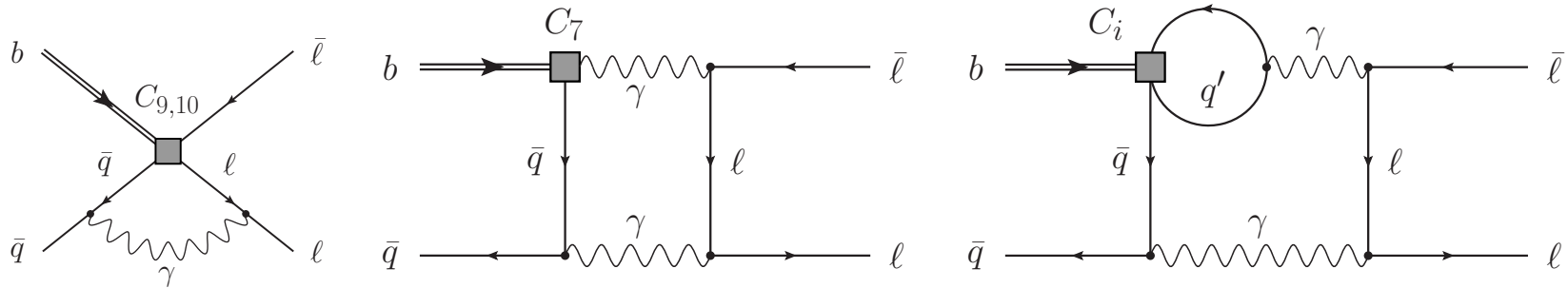
$$\eta_{\text{QED}} = 0.995_{-0.05}^{+0.03}.$$

Enhanced QED effects in $B_q \rightarrow \ell^+ \ell^-$

The leading contribution to the decay rate is suppressed by $\frac{m_\ell^2}{M_{Bq}^2}$.

As observed by M. Beneke, C. Bobeth and R. Szafron in arXiv:1708.09152,

some of the QED corrections receive suppression by $\frac{m_\ell^2}{\Lambda M_{Bq}}$ only:



See also the lecture by RS at the Paris-2019 workshop:

<https://indico.in2p3.fr/event/18845/sessions/12137/attachments/54326/71064/Szafron.pdf>

Consequently, the relative QED correction scales like $\frac{\alpha_{em}}{\pi} \frac{M_{Bq}}{\Lambda}$.

Their explicit calculation in arXiv:1908.07011 implies that the previous results for all the $B_q \rightarrow \ell^+ \ell^-$ branching ratios need to be multiplied by

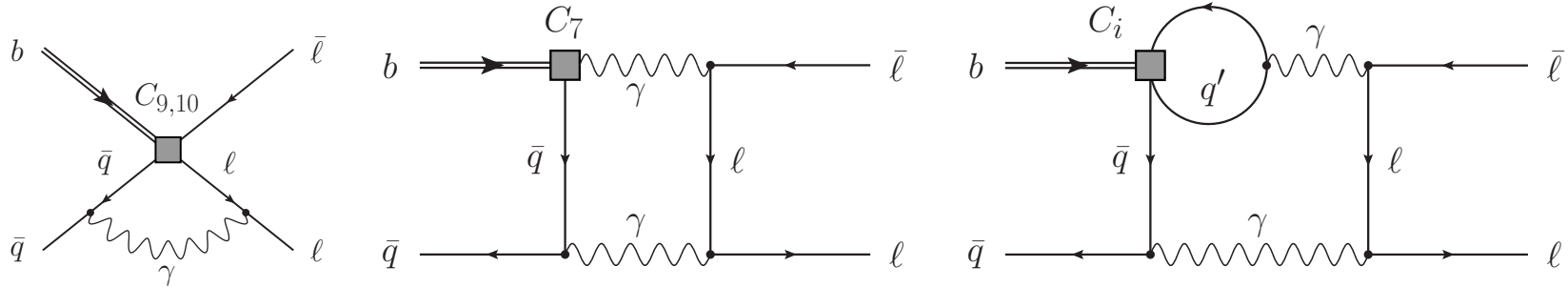
$$\eta_{\text{QED}} = 0.995^{+0.03}_{-0.05}.$$

Thus, despite the $\frac{M_{Bq}}{\Lambda}$ -enhancement, the effect is well within the previously estimated $\pm 1.5\%$ non-parametric uncertainty.

Enhanced QED effects in $B_q \rightarrow \ell^+ \ell^-$

The leading contribution to the decay rate is suppressed by $\frac{m_\ell^2}{M_{B_q}^2}$.

As observed by M. Beneke, C. Bobeth and R. Szafron in arXiv:1708.09152, some of the QED corrections receive suppression by $\frac{m_\ell^2}{\Lambda M_{B_q}}$ only:



See also the lecture by RS at the Paris-2019 workshop:

<https://indico.in2p3.fr/event/18845/sessions/12137/attachments/54326/71064/Szafron.pdf>

Consequently, the relative QED correction scales like $\frac{\alpha_{em}}{\pi} \frac{M_{B_q}}{\Lambda}$.

Their explicit calculation in arXiv:1908.07011 implies that the previous results for all the $B_q \rightarrow \ell^+ \ell^-$ branching ratios need to be multiplied by

$$\eta_{\text{QED}} = 0.995^{+0.03}_{-0.05}.$$

Thus, despite the $\frac{M_{B_q}}{\Lambda}$ -enhancement, the effect is well within the previously estimated $\pm 1.5\%$ non-parametric uncertainty.

However, it is larger than $\pm 0.3\%$ due to scale-variation of the Wilson coefficient $C_A(\mu_b)$.

Determination of $\mathcal{B}(\bar{B} \rightarrow X_s \gamma)$ in the SM:

$$\mathcal{B}(\bar{B} \rightarrow X_s \gamma)_{E_\gamma > E_0} = \mathcal{B}(\bar{B} \rightarrow X_c e \bar{\nu})_{\text{exp}} \left| \frac{V_{ts}^* V_{tb}}{V_{cb}} \right|^2 \frac{6\alpha_{\text{em}}}{\pi} \mathbf{C} \left[\underset{\substack{\text{pert.} \\ \sim 96\%}}{\mathbf{P}(\mathbf{E}_0)} + \underset{\substack{\text{non-pert.} \\ \sim 4\%}}{N(E_0)} \right]$$

$$\frac{\Gamma[b \rightarrow X_s^p \gamma]_{E_\gamma > E_0}}{|V_{cb}/V_{ub}|^2 \Gamma[b \rightarrow X_u^p e \bar{\nu}]} = \left| \frac{V_{ts}^* V_{tb}}{V_{cb}} \right|^2 \frac{6\alpha_{\text{em}}}{\pi} \mathbf{P}(\mathbf{E}_0)$$

$$\mathbf{C} = \left| \frac{V_{ub}}{V_{cb}} \right|^2 \frac{\Gamma[\bar{B} \rightarrow X_c e \bar{\nu}]}{\Gamma[\bar{B} \rightarrow X_u e \bar{\nu}]}$$

semileptonic phase-space factor

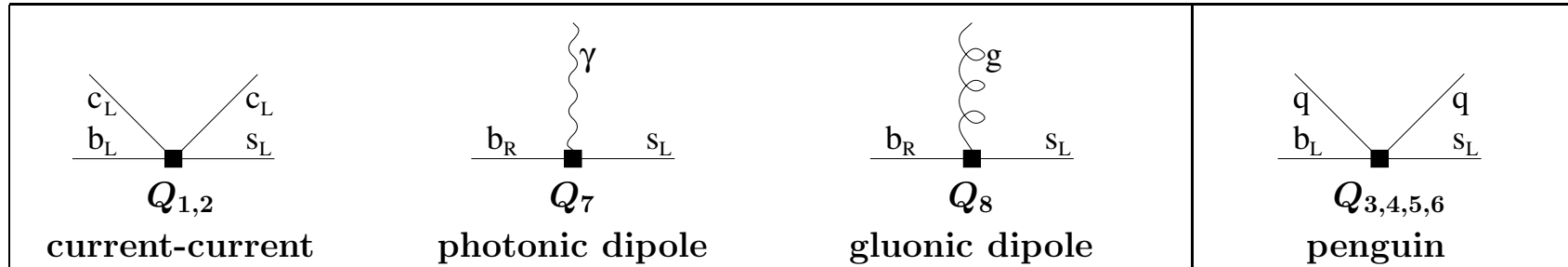
Determination of $\mathcal{B}(\bar{B} \rightarrow X_s \gamma)$ in the SM:

$$\mathcal{B}(\bar{B} \rightarrow X_s \gamma)_{E_\gamma > E_0} = \mathcal{B}(\bar{B} \rightarrow X_c e \bar{\nu})_{\text{exp}} \left| \frac{V_{ts}^* V_{tb}}{V_{cb}} \right|^2 \frac{6\alpha_{\text{em}}}{\pi} \mathcal{C} [\underbrace{\mathbf{P}(\mathbf{E}_0)}_{\substack{\text{pert.} \\ \sim 96\%}} + \underbrace{N(E_0)}_{\substack{\text{non-pert.} \\ \sim 4\%}}]$$

$$\frac{\Gamma[b \rightarrow X_s^p \gamma]_{E_\gamma > E_0}}{|V_{cb}/V_{ub}|^2 \Gamma[b \rightarrow X_u^p e \bar{\nu}]} = \left| \frac{V_{ts}^* V_{tb}}{V_{cb}} \right|^2 \frac{6\alpha_{\text{em}}}{\pi} \mathbf{P}(\mathbf{E}_0) \quad \mathcal{C} = \left| \frac{V_{ub}}{V_{cb}} \right|^2 \frac{\Gamma[\bar{B} \rightarrow X_c e \bar{\nu}]}{\Gamma[\bar{B} \rightarrow X_u e \bar{\nu}]}$$

semileptonic phase-space factor

Eight operators Q_i matter for $\mathcal{B}_{s\gamma}^{\text{SM}}$ when the NLO EW and/or CKM-suppressed effects are neglected:



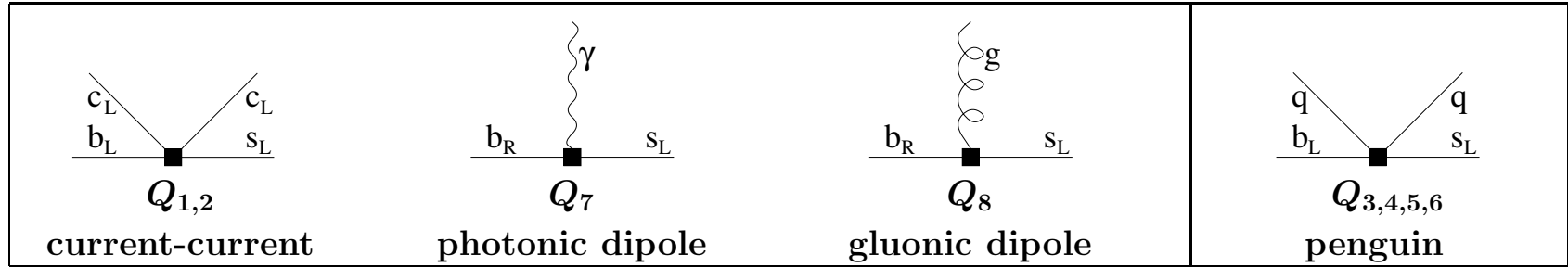
Determination of $\mathcal{B}(\bar{B} \rightarrow X_s \gamma)$ in the SM:

$$\mathcal{B}(\bar{B} \rightarrow X_s \gamma)_{E_\gamma > E_0} = \mathcal{B}(\bar{B} \rightarrow X_c e \bar{\nu})_{\text{exp}} \left| \frac{V_{ts}^* V_{tb}}{V_{cb}} \right|^2 \frac{6\alpha_{\text{em}}}{\pi} \underbrace{\mathbf{P}(\mathbf{E}_0)}_{\substack{\text{pert.} \\ \sim 96\%}} + \underbrace{N(E_0)}_{\substack{\text{non-pert.} \\ \sim 4\%}}$$

$$\frac{\Gamma[b \rightarrow X_s^p \gamma]_{E_\gamma > E_0}}{|V_{cb}/V_{ub}|^2 \Gamma[b \rightarrow X_u^p e \bar{\nu}]} = \left| \frac{V_{ts}^* V_{tb}}{V_{cb}} \right|^2 \frac{6\alpha_{\text{em}}}{\pi} \mathbf{P}(\mathbf{E}_0) \quad \mathbf{C} = \left| \frac{V_{ub}}{V_{cb}} \right|^2 \frac{\Gamma[\bar{B} \rightarrow X_c e \bar{\nu}]}{\Gamma[\bar{B} \rightarrow X_u e \bar{\nu}]}$$

semileptonic phase-space factor

Eight operators Q_i matter for $\mathcal{B}_{s\gamma}^{\text{SM}}$ when the NLO EW and/or CKM-suppressed effects are neglected:



$$\Gamma(b \rightarrow X_s^p \gamma) = \frac{G_F^2 m_{b, \text{pole}}^5 \alpha_{em}}{32\pi^4} |V_{ts}^* V_{tb}|^2 \sum_{i,j=1}^8 C_i(\mu_b) C_j(\mu_b) \hat{G}_{ij}, \quad (\hat{G}_{ij} = \hat{G}_{ji})$$

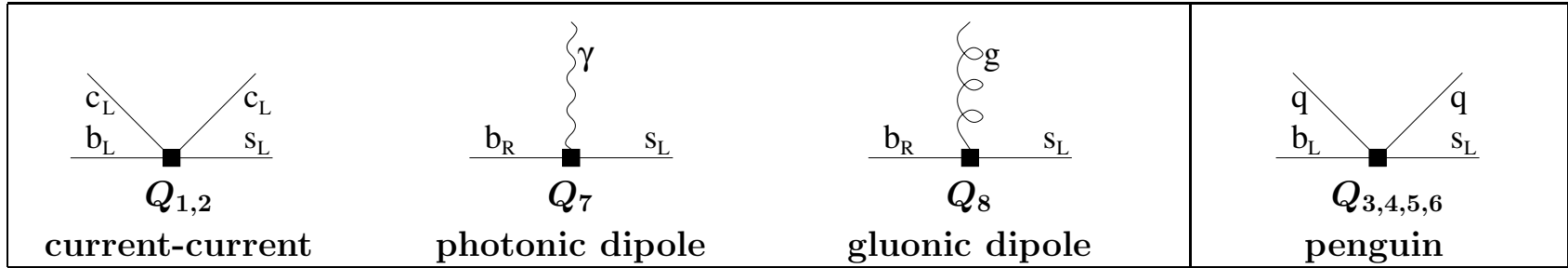
Determination of $\mathcal{B}(\bar{B} \rightarrow X_s \gamma)$ in the SM:

$$\mathcal{B}(\bar{B} \rightarrow X_s \gamma)_{E_\gamma > E_0} = \mathcal{B}(\bar{B} \rightarrow X_c e \bar{\nu})_{\text{exp}} \left| \frac{V_{ts}^* V_{tb}}{V_{cb}} \right|^2 \frac{6\alpha_{\text{em}}}{\pi} \underbrace{\mathbf{P}(\mathbf{E}_0)}_{\substack{\text{pert.} \\ \sim 96\%}} + \underbrace{N(E_0)}_{\substack{\text{non-pert.} \\ \sim 4\%}}$$

$$\frac{\Gamma[b \rightarrow X_s^p \gamma]_{E_\gamma > E_0}}{|V_{cb}/V_{ub}|^2 \Gamma[b \rightarrow X_u^p e \bar{\nu}]} = \left| \frac{V_{ts}^* V_{tb}}{V_{cb}} \right|^2 \frac{6\alpha_{\text{em}}}{\pi} \mathbf{P}(\mathbf{E}_0) \quad \mathbf{C} = \left| \frac{V_{ub}}{V_{cb}} \right|^2 \frac{\Gamma[\bar{B} \rightarrow X_c e \bar{\nu}]}{\Gamma[\bar{B} \rightarrow X_u e \bar{\nu}]}$$

semileptonic phase-space factor

Eight operators Q_i matter for $\mathcal{B}_{s\gamma}^{\text{SM}}$ when the NLO EW and/or CKM-suppressed effects are neglected:



$$\Gamma(b \rightarrow X_s^p \gamma) = \frac{G_F^2 m_{b, \text{pole}}^5 \alpha_{\text{em}}}{32\pi^4} |V_{ts}^* V_{tb}|^2 \sum_{i,j=1}^8 C_i(\mu_b) C_j(\mu_b) \hat{G}_{ij}, \quad (\hat{G}_{ij} = \hat{G}_{ji})$$

NLO ($\mathcal{O}(\alpha_s)$) – last missing pieces being evaluated by Tobias Huber and Lars-Thorben Moos

[arXiv:1912.07916]

Most important @ NNLO ($\mathcal{O}(\alpha_s^2)$): \hat{G}_{77} , \hat{G}_{17} , \hat{G}_{27}

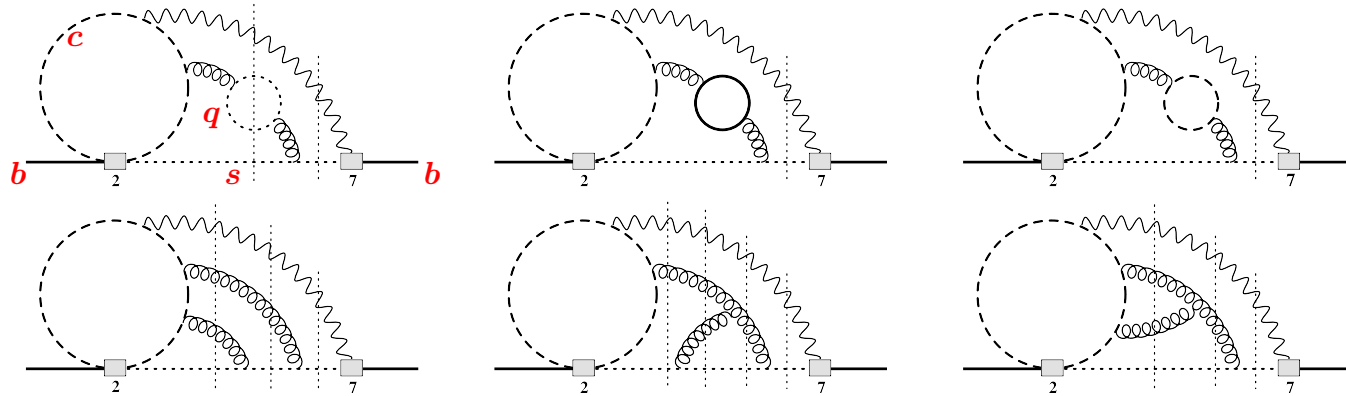
known

interpolated

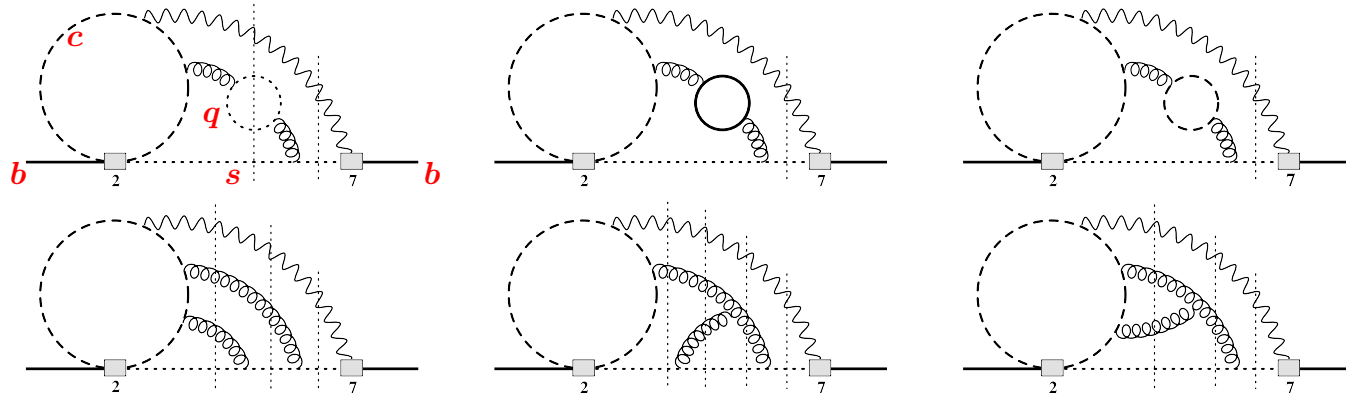
between the $m_c \gg m_b$ and $m_c = 0$ limits [arXiv:1503.01791]

$\Rightarrow \pm 3\%$ uncertainty in $\mathcal{B}_{s\gamma}^{\text{SM}}$

Sample diagrams contributing to \hat{G}_{27} @ NNLO:

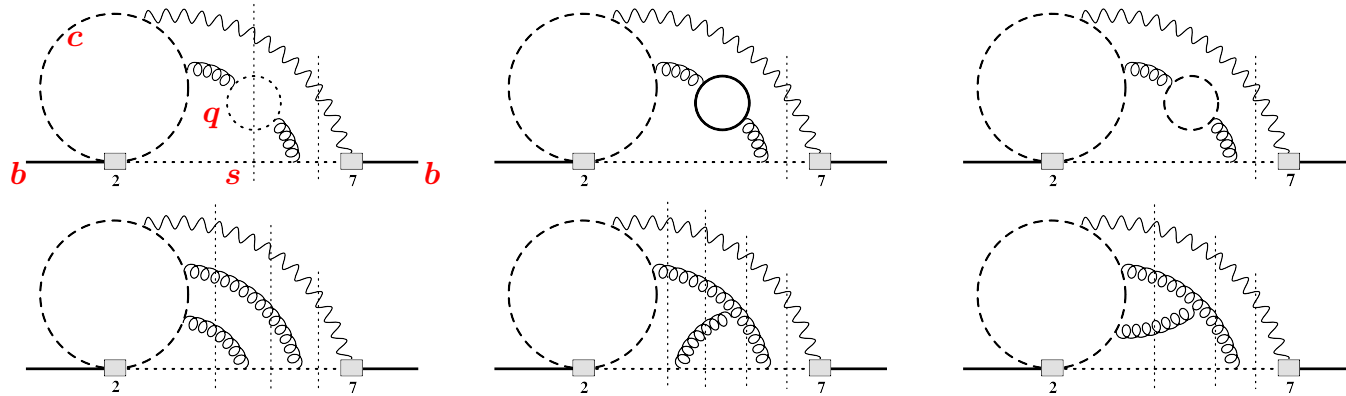


Sample diagrams contributing to \hat{G}_{27} @ NNLO:



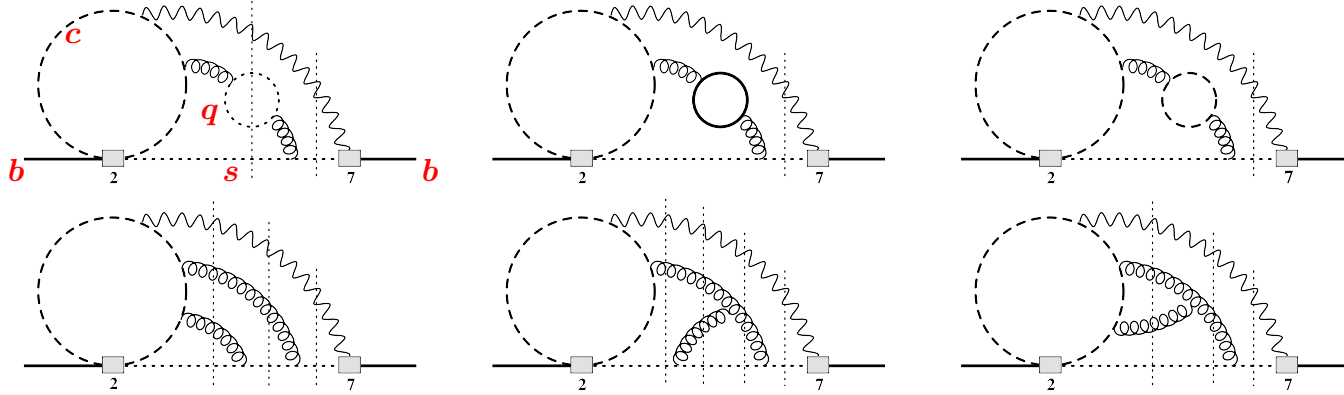
1. Generation of diagrams and performing the Dirac algebra to express everything in terms of (a few) $\times 10^5$ **four-loop** **two-scale** scalar integrals with unitarity cuts ($\mathcal{O}(500)$ families).

Sample diagrams contributing to \hat{G}_{27} @ NNLO:



1. Generation of diagrams and performing the Dirac algebra to express everything in terms of (a few) $\times 10^5$ **four-loop** **two-scale** scalar integrals with unitarity cuts ($\mathcal{O}(500)$ families).
2. Reduction to master integrals with the help of Integration By Parts (IBP) [KIRA]. $\mathcal{O}(1 \text{ TB})$ RAM and weeks of CPU needed for the most complicated families.

Sample diagrams contributing to \hat{G}_{27} @ NNLO:

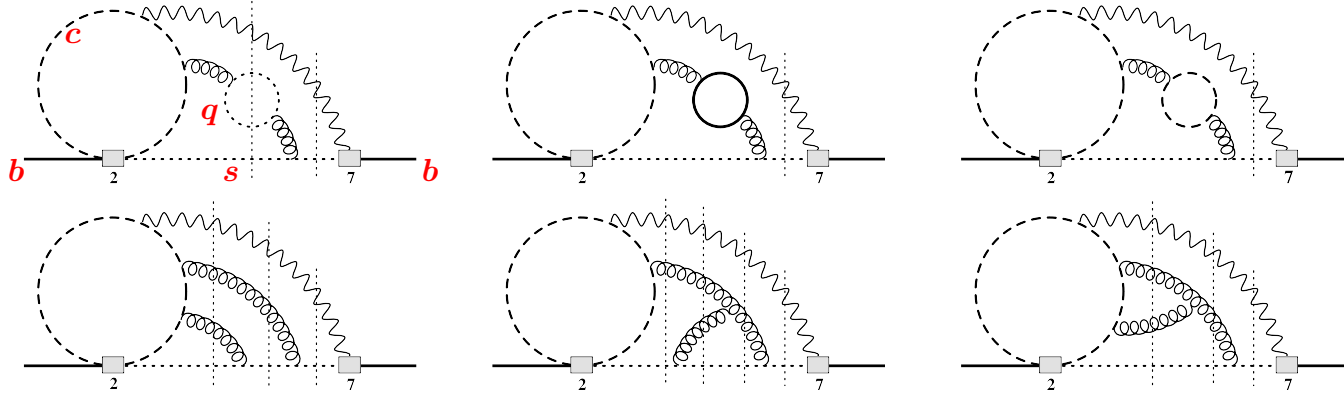


1. Generation of diagrams and performing the Dirac algebra to express everything in terms of (a few) $\times 10^5$ **four-loop two-scale** scalar integrals with unitarity cuts ($\mathcal{O}(500)$ families).
2. Reduction to master integrals with the help of Integration By Parts (IBP) [KIRA]. $\mathcal{O}(1 \text{ TB})$ RAM and weeks of CPU needed for the most complicated families.
3. Extending the set of master integrals M_k so that it closes under differentiation with respect to $z = m_c^2/m_b^2$. This way one obtains a system of differential equations

$$\frac{d}{dz} M_k(z, \epsilon) = \sum_l R_{kl}(z, \epsilon) M_l(z, \epsilon), \quad (*)$$

where R_{nk} are rational functions of their arguments.

Sample diagrams contributing to \hat{G}_{27} @ NNLO:



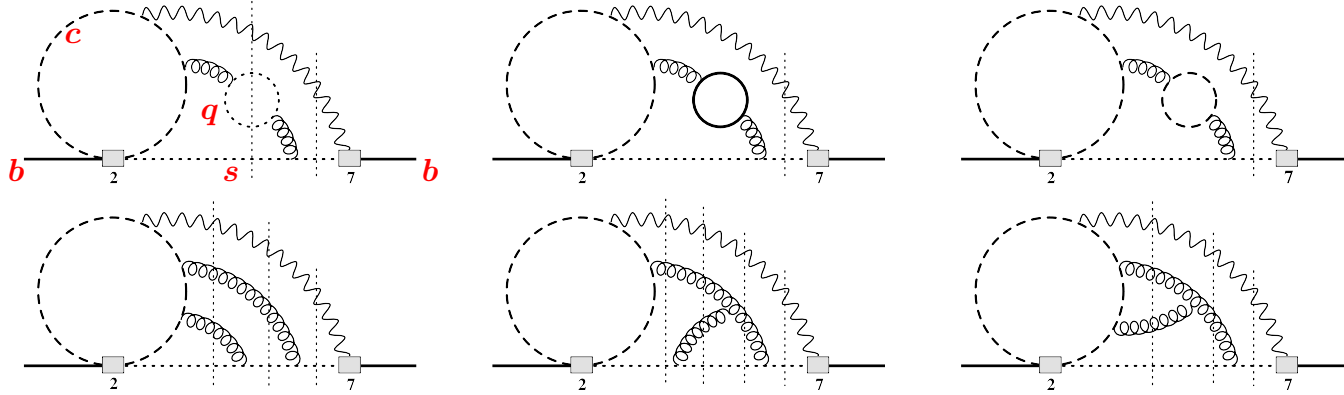
1. Generation of diagrams and performing the Dirac algebra to express everything in terms of (a few) $\times 10^5$ **four-loop two-scale** scalar integrals with unitarity cuts ($\mathcal{O}(500)$ families).
2. Reduction to master integrals with the help of Integration By Parts (IBP) [KIRA]. $\mathcal{O}(1 \text{ TB})$ RAM and weeks of CPU needed for the most complicated families.
3. Extending the set of master integrals M_k so that it closes under differentiation with respect to $z = m_c^2/m_b^2$. This way one obtains a system of differential equations

$$\frac{d}{dz} M_k(z, \epsilon) = \sum_l R_{kl}(z, \epsilon) M_l(z, \epsilon), \quad (*)$$

where R_{nk} are rational functions of their arguments.

4. Calculating boundary conditions for (*) using automatized asymptotic expansions at $m_c \gg m_b$.

Sample diagrams contributing to \hat{G}_{27} @ NNLO:



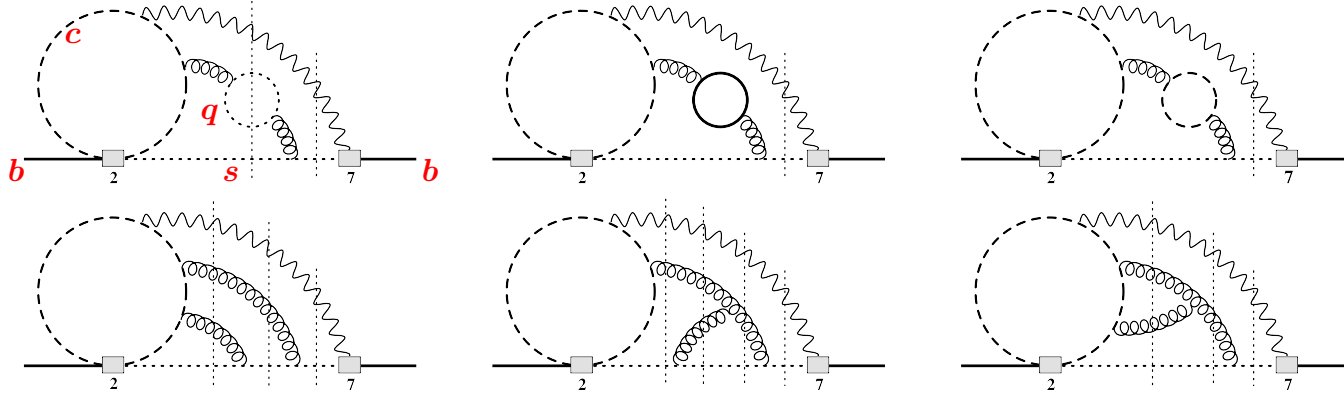
1. Generation of diagrams and performing the Dirac algebra to express everything in terms of (a few) $\times 10^5$ **four-loop two-scale** scalar integrals with unitarity cuts ($\mathcal{O}(500)$ families).
2. Reduction to master integrals with the help of Integration By Parts (IBP) [KIRA]. $\mathcal{O}(1 \text{ TB})$ RAM and weeks of CPU needed for the most complicated families.
3. Extending the set of master integrals M_k so that it closes under differentiation with respect to $z = m_c^2/m_b^2$. This way one obtains a system of differential equations

$$\frac{d}{dz} M_k(z, \epsilon) = \sum_l R_{kl}(z, \epsilon) M_l(z, \epsilon), \quad (*)$$

where R_{nk} are rational functions of their arguments.

4. Calculating boundary conditions for (*) using automatized asymptotic expansions at $m_c \gg m_b$.
5. Calculating **three-loop single-scale** master integrals for the boundary conditions.

Sample diagrams contributing to \hat{G}_{27} @ NNLO:



1. Generation of diagrams and performing the Dirac algebra to express everything in terms of (a few) $\times 10^5$ **four-loop two-scale** scalar integrals with unitarity cuts ($\mathcal{O}(500)$ families).
2. Reduction to master integrals with the help of Integration By Parts (IBP) [KIRA]. $\mathcal{O}(1 \text{ TB})$ RAM and weeks of CPU needed for the most complicated families.
3. Extending the set of master integrals M_k so that it closes under differentiation with respect to $z = m_c^2/m_b^2$. This way one obtains a system of differential equations

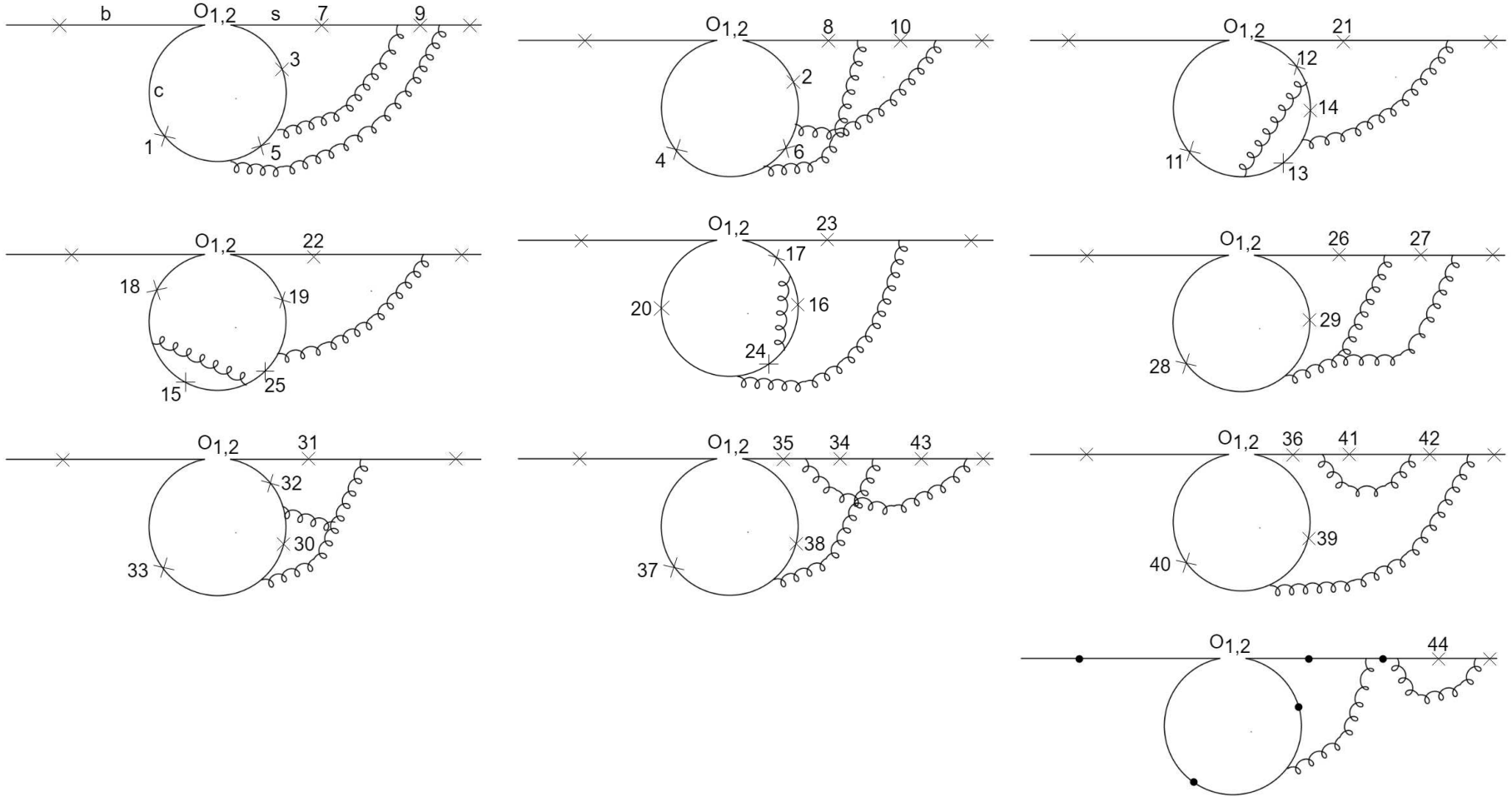
$$\frac{d}{dz} M_k(z, \epsilon) = \sum_l R_{kl}(z, \epsilon) M_l(z, \epsilon), \quad (*)$$

where R_{nk} are rational functions of their arguments.

4. Calculating boundary conditions for (*) using automatized asymptotic expansions at $m_c \gg m_b$.
5. Calculating **three-loop single-scale** master integrals for the boundary conditions.
6. Solving the system (*) numerically [A.C. Hindmarch, <http://www.netlib.org/odepack>] along an ellipse in the complex z plane. Doing so along several different ellipses allows us to estimate the numerical error.

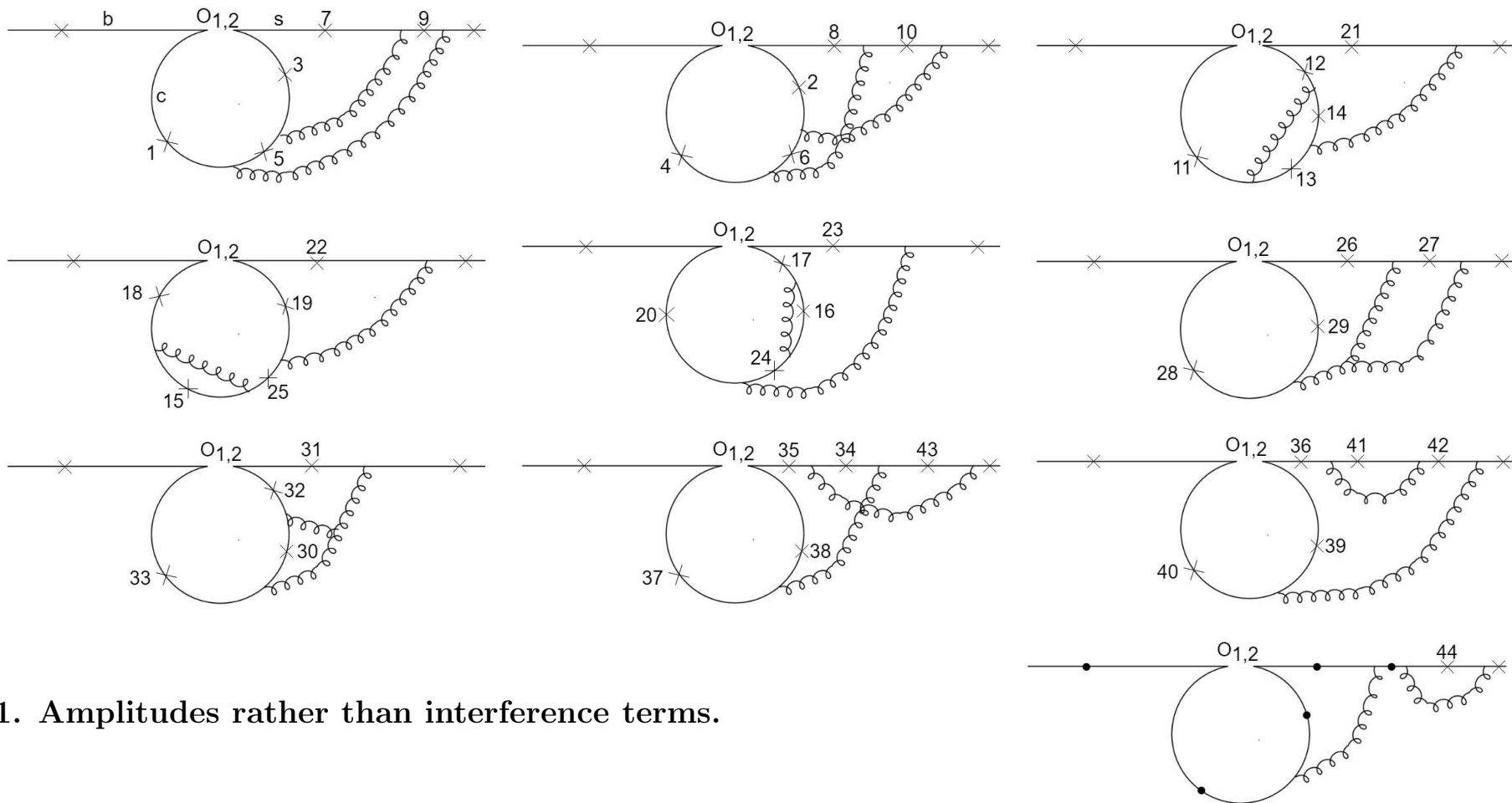
Another approach to bare 2-body contributions in arXiv:2303.01714

[C. Greub, H.M. Asatrian, F. Saturnino, C. Wiegand]



Another approach to bare 2-body contributions in arXiv:2303.01714

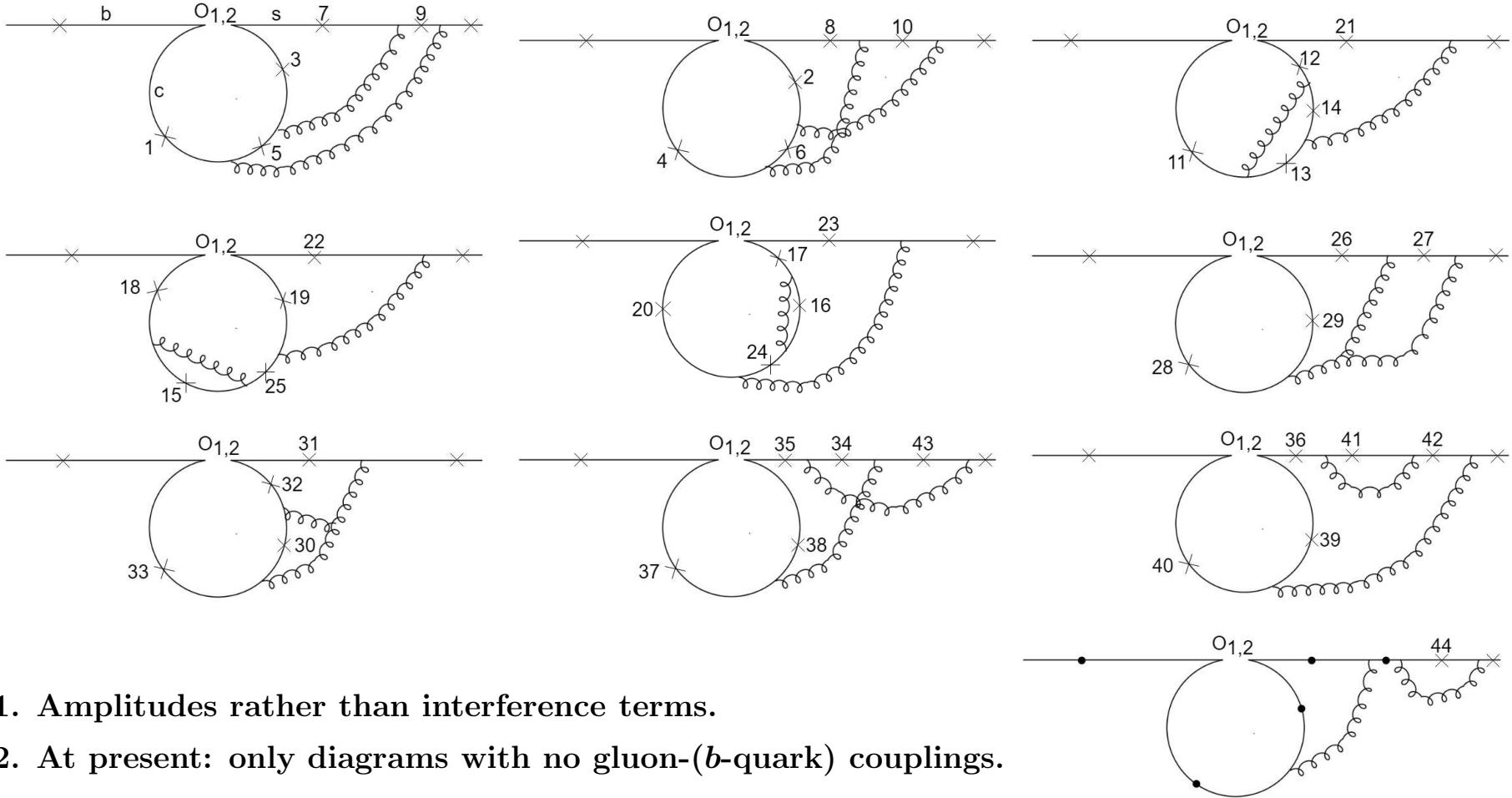
[C. Greub, H.M. Asatrian, F. Saturnino, C. Wiegand]



1. Amplitudes rather than interference terms.

Another approach to bare 2-body contributions in arXiv:2303.01714

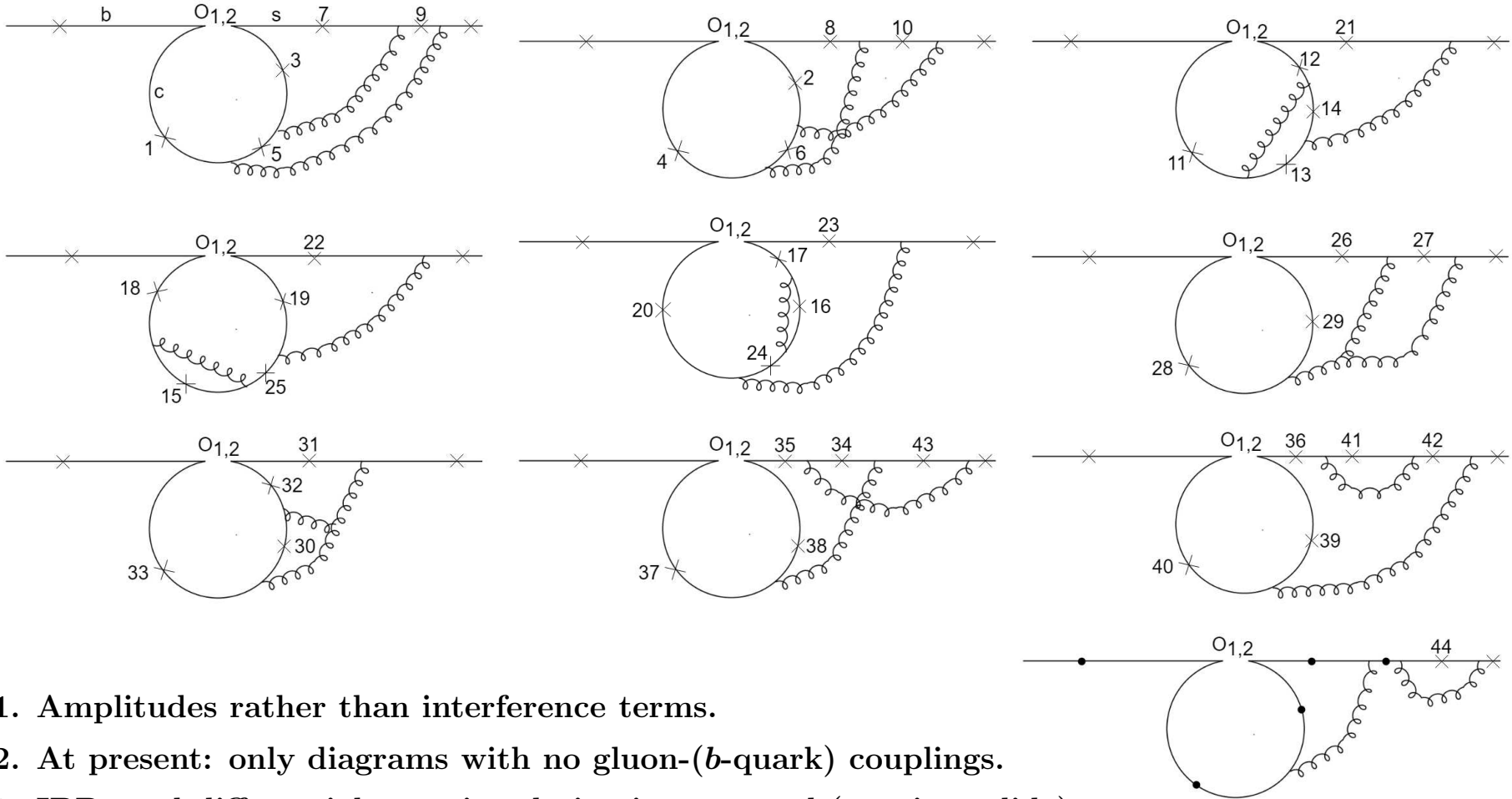
[C. Greub, H.M. Asatrian, F. Saturnino, C. Wiegand]



1. Amplitudes rather than interference terms.
2. At present: only diagrams with no gluon-(b -quark) couplings.

Another approach to bare 2-body contributions in arXiv:2303.01714

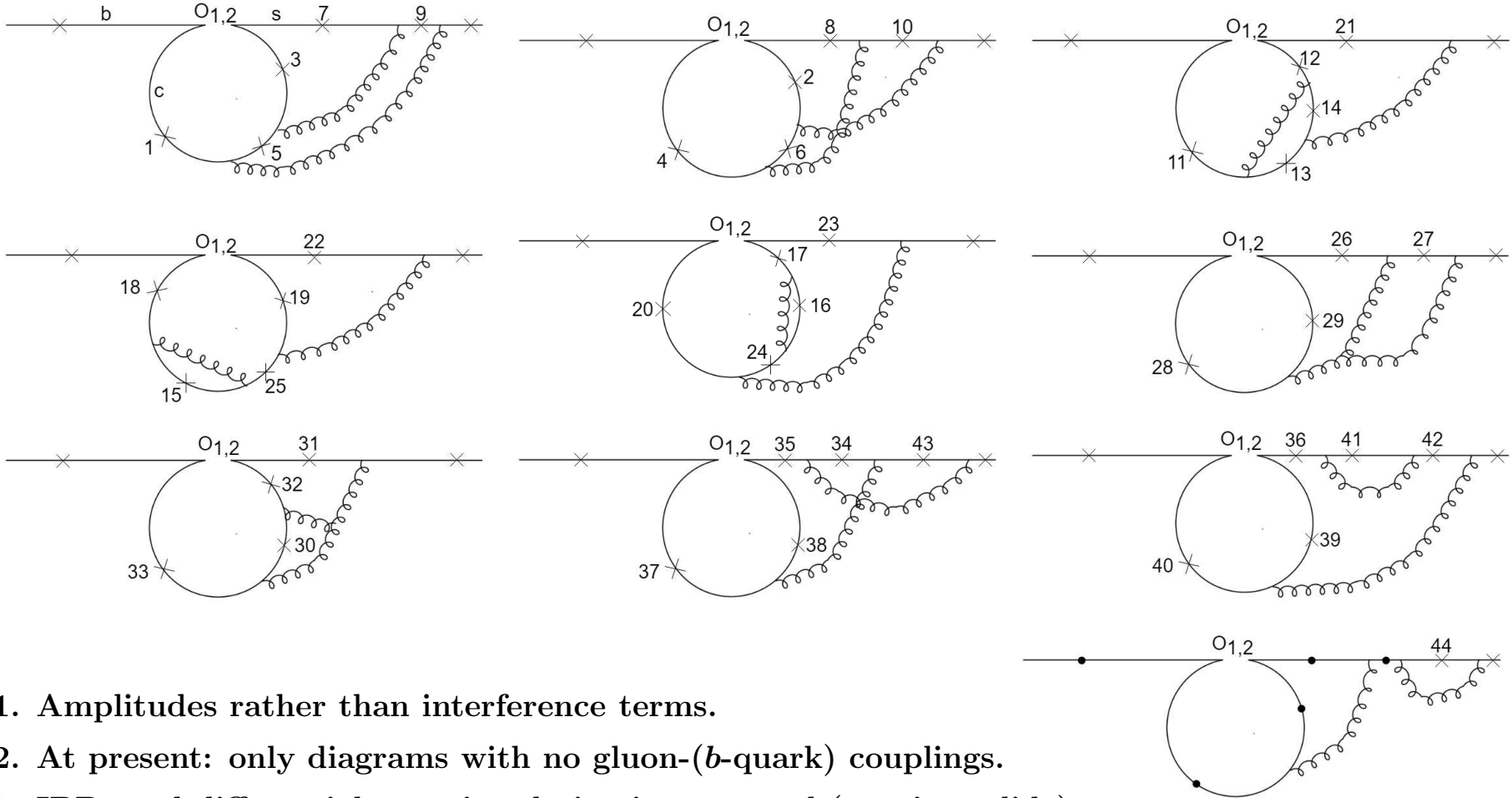
[C. Greub, H.M. Asatrian, F. Saturnino, C. Wiegand]



1. Amplitudes rather than interference terms.
2. At present: only diagrams with no gluon-(b -quark) couplings.
3. IBPs and differential equation derivation as usual (previous slide).

Another approach to bare 2-body contributions in arXiv:2303.01714

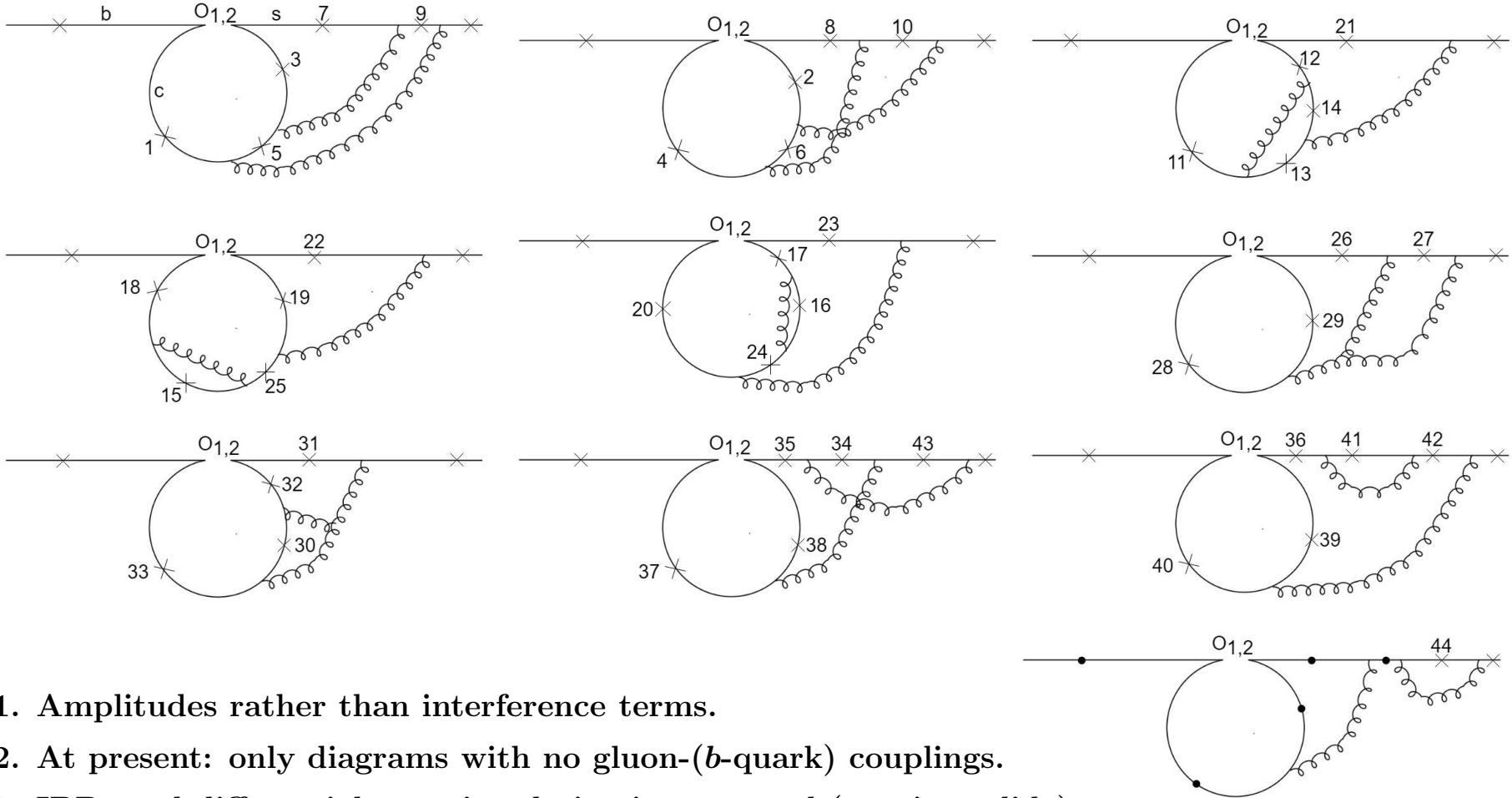
[C. Greub, H.M. Asatrian, F. Saturnino, C. Wiegand]



1. Amplitudes rather than interference terms.
2. At present: only diagrams with no gluon- $(b\text{-quark})$ couplings.
3. IBPs and differential equation derivation as usual (previous slide).
4. Transforming the differential equations to the canonical form (CANONICA) and solving them analytically in terms of Harmonic Polylogarithms for 8 out of 10 diagram classes.

Another approach to bare 2-body contributions in arXiv:2303.01714

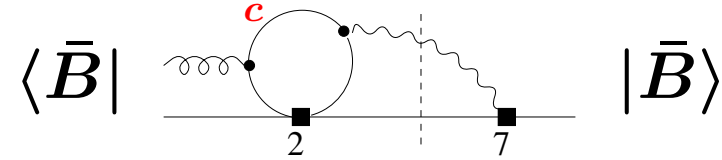
[C. Greub, H.M. Asatrian, F. Saturnino, C. Wiegand]



1. Amplitudes rather than interference terms.
2. At present: only diagrams with no gluon- $(b\text{-quark})$ couplings.
3. IBPs and differential equation derivation as usual (previous slide).
4. Transforming the differential equations to the canonical form (CANONICA) and solving them analytically in terms of Harmonic Polylogarithms for 8 out of 10 diagram classes.
5. Numerical solutions in the remaining 2 cases.

Resolved photon contribution to the Q_7 - $Q_{1,2}$ interference.

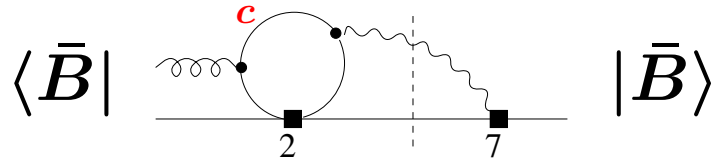
M.B. Voloshin, hep-ph/9612483; A. Khodjamirian, R. Rückl, G. Stoll and D. Wyler, hep-ph/9702318;
 Z. Ligeti, L. Randall and M.B. Wise, hep-ph/9702322; G. Buchalla, G. Isidori, G. Rey, [hep-ph/9705253](#);
 M. Benzke, S.J. Lee, M. Neubert, G. Paz, arXiv:1003.5012; A. Gunawardana, G. Paz, [arXiv:1908.02812](#).



$$\delta \mathbf{N}(\mathbf{E}_0) = (C_2 - \frac{1}{6}C_1)C_7 \left[\underbrace{-\frac{\mu_G^2}{27m_c^2} + \frac{\Lambda_{17}}{m_b}}_{-\frac{\kappa_V \mu_G^2}{27m_c^2}} \right]$$

Resolved photon contribution to the Q_7 - $Q_{1,2}$ interference.

M.B. Voloshin, hep-ph/9612483; A. Khodjamirian, R. Rückl, G. Stoll and D. Wyler, hep-ph/9702318;
 Z. Ligeti, L. Randall and M.B. Wise, hep-ph/9702322; G. Buchalla, G. Isidori, G. Rey, [hep-ph/9705253](#);
 M. Benzke, S.J. Lee, M. Neubert, G. Paz, arXiv:1003.5012; A. Gunawardana, G. Paz, [arXiv:1908.02812](#).



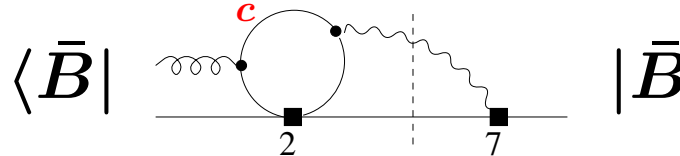
$$\delta \mathbf{N}(\mathbf{E}_0) = (C_2 - \frac{1}{6}C_1)C_7 \left[\underbrace{-\frac{\mu_G^2}{27m_c^2} + \frac{\Lambda_{17}}{m_b}}_{-\frac{\kappa_V \mu_G^2}{27m_c^2}} \right]$$

$$\Lambda_{17} = \frac{2}{3} \text{Re} \int_{-\infty}^{\infty} \frac{d\omega_1}{\omega_1} \left[1 - F \left(\frac{m_c^2 - i\varepsilon}{m_b \omega_1} \right) + \frac{m_b \omega_1}{12m_c^2} \right] h_{17}(\omega_1, \mu)$$

$$\omega_1 \leftrightarrow \text{gluon momentum}, \quad F(x) = 4x \arctan^2(1/\sqrt{4x-1})$$

Resolved photon contribution to the Q_7 - $Q_{1,2}$ interference.

M.B. Voloshin, hep-ph/9612483; A. Khodjamirian, R. Rückl, G. Stoll and D. Wyler, hep-ph/9702318;
 Z. Ligeti, L. Randall and M.B. Wise, hep-ph/9702322; G. Buchalla, G. Isidori, G. Rey, [hep-ph/9705253](#);
 M. Benzke, S.J. Lee, M. Neubert, G. Paz, arXiv:1003.5012; A. Gunawardana, G. Paz, [arXiv:1908.02812](#).



$$\delta\mathbf{N}(\mathbf{E}_0) = (C_2 - \frac{1}{6}C_1)C_7 \left[\underbrace{-\frac{\mu_G^2}{27m_c^2} + \frac{\Lambda_{17}}{m_b}}_{-\frac{\kappa_V\mu_G^2}{27m_c^2}} \right]$$

$$\Lambda_{17} = \frac{2}{3}\text{Re} \int_{-\infty}^{\infty} \frac{d\omega_1}{\omega_1} \left[1 - F \left(\frac{m_c^2 - i\varepsilon}{m_b\omega_1} \right) + \frac{m_b\omega_1}{12m_c^2} \right] h_{17}(\omega_1, \mu)$$

$$\omega_1 \leftrightarrow \text{gluon momentum}, \quad F(x) = 4x \arctan^2(1/\sqrt{4x-1})$$

The soft function h_{17} :

$$h_{17}(\omega_1, \mu) = \int \frac{dr}{4\pi M_B} e^{-i\omega_1 r} \langle \bar{B} | (\bar{h}S_{\bar{n}})(0) \not{n} i\gamma_{\alpha}^{\perp} \bar{n}_{\beta} (S_{\bar{n}}^{\dagger} g G_s^{\alpha\beta} S_{\bar{n}})(r\bar{n}) (S_{\bar{n}}^{\dagger} h)(0) | \bar{B} \rangle \quad (m_b - 2E_0 \gg \Lambda_{\text{QCD}})$$

A class of models for h_{17} :

$$h_{17}(\omega_1, \mu) = e^{-\frac{\omega_1^2}{2\sigma^2}} \sum_n a_{2n} H_{2n} \left(\frac{\omega_1}{\sigma\sqrt{2}} \right), \quad \sigma < 1 \text{ GeV}$$

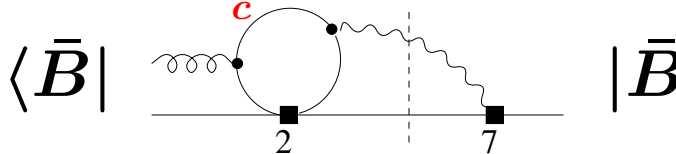
Hermite polynomials

Constraints on moments (e.g.):

$$\int d\omega_1 h_{17} = \frac{2}{3}\mu_G^2, \quad \int d\omega_1 \omega_1^2 h_{17} = \frac{2}{15}(5m_5 + 3m_6 - 2m_9).$$

Resolved photon contribution to the Q_7 - $Q_{1,2}$ interference.

M.B. Voloshin, hep-ph/9612483; A. Khodjamirian, R. Rückl, G. Stoll and D. Wyler, hep-ph/9702318;
 Z. Ligeti, L. Randall and M.B. Wise, hep-ph/9702322; G. Buchalla, G. Isidori, G. Rey, [hep-ph/9705253](#);
 M. Benzke, S.J. Lee, M. Neubert, G. Paz, arXiv:1003.5012; A. Gunawardana, G. Paz, [arXiv:1908.02812](#).



$$\delta N(E_0) = (C_2 - \frac{1}{6}C_1)C_7 \left[\underbrace{-\frac{\mu_G^2}{27m_c^2} + \frac{\Lambda_{17}}{m_b}}_{-\frac{\kappa_V \mu_G^2}{27m_c^2}} \right]$$

$$\Lambda_{17} = \frac{2}{3} \text{Re} \int_{-\infty}^{\infty} \frac{d\omega_1}{\omega_1} \left[1 - F \left(\frac{m_c^2 - i\varepsilon}{m_b \omega_1} \right) + \frac{m_b \omega_1}{12m_c^2} \right] h_{17}(\omega_1, \mu)$$

$$\omega_1 \leftrightarrow \text{gluon momentum}, \quad F(x) = 4x \arctan^2(1/\sqrt{4x-1})$$

The soft function h_{17} :

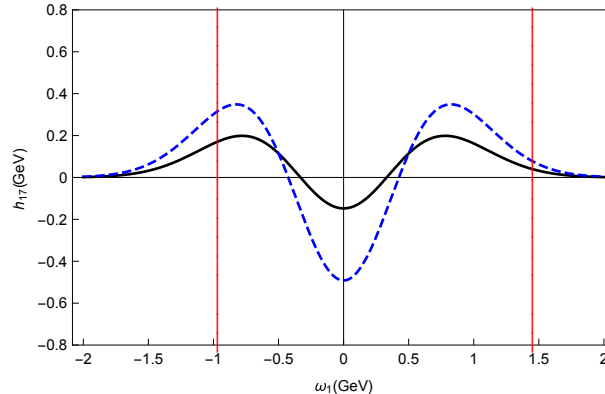
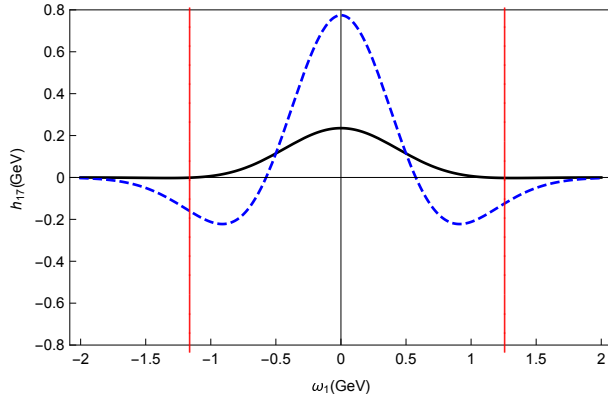
$$h_{17}(\omega_1, \mu) = \int \frac{dr}{4\pi M_B} e^{-i\omega_1 r} \langle \bar{B} | (\bar{h} S_{\bar{n}})(0) \not{n} i\gamma_{\alpha}^{\perp} \bar{n}_{\beta} (S_n^{\dagger} g G_s^{\alpha\beta} S_n)(r\bar{n}) (S_n^{\dagger} h)(0) | \bar{B} \rangle \quad (m_b - 2E_0 \gg \Lambda_{\text{QCD}})$$

A class of models for h_{17} :

$$h_{17}(\omega_1, \mu) = e^{-\frac{\omega_1^2}{2\sigma^2}} \sum_n a_{2n} H_{2n} \left(\frac{\omega_1}{\sigma\sqrt{2}} \right), \quad \sigma < 1 \text{ GeV}$$

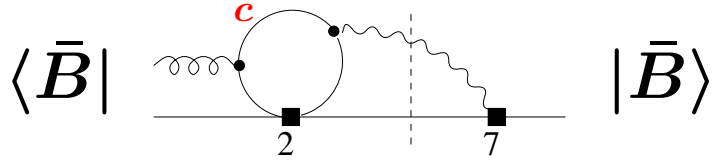
Hermite polynomials

Constraints on moments (e.g.): $\int d\omega_1 h_{17} = \frac{2}{3}\mu_G^2, \quad \int d\omega_1 \omega_1^2 h_{17} = \frac{2}{15}(5m_5 + 3m_6 - 2m_9).$



Resolved photon contribution to the Q_7 - $Q_{1,2}$ interference.

M.B. Voloshin, hep-ph/9612483; A. Khodjamirian, R. Rückl, G. Stoll and D. Wyler, hep-ph/9702318;
 Z. Ligeti, L. Randall and M.B. Wise, hep-ph/9702322; G. Buchalla, G. Isidori, G. Rey, [hep-ph/9705253](#);
 M. Benzke, S.J. Lee, M. Neubert, G. Paz, arXiv:1003.5012; A. Gunawardana, G. Paz, [arXiv:1908.02812](#).



$$\delta N(E_0) = (C_2 - \frac{1}{6}C_1)C_7 \left[\underbrace{-\frac{\mu_G^2}{27m_c^2} + \frac{\Lambda_{17}}{m_b}}_{-\frac{\kappa_V \mu_G^2}{27m_c^2}} \right]$$

$$\Lambda_{17} = \frac{2}{3} \text{Re} \int_{-\infty}^{\infty} \frac{d\omega_1}{\omega_1} \left[1 - F \left(\frac{m_c^2 - i\varepsilon}{m_b \omega_1} \right) + \frac{m_b \omega_1}{12m_c^2} \right] h_{17}(\omega_1, \mu)$$

$$\omega_1 \leftrightarrow \text{gluon momentum}, \quad F(x) = 4x \arctan^2(1/\sqrt{4x-1})$$

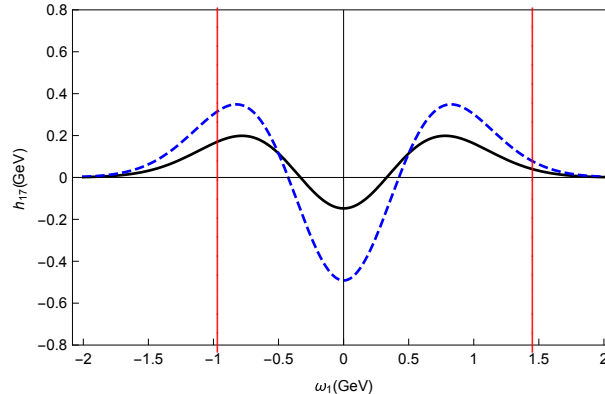
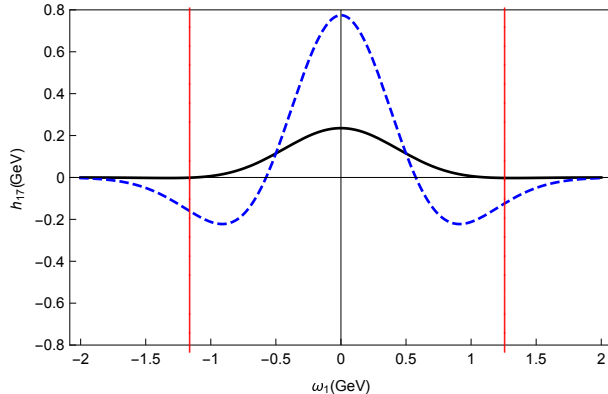
The soft function h_{17} :

$$h_{17}(\omega_1, \mu) = \int \frac{dr}{4\pi M_B} e^{-i\omega_1 r} \langle \bar{B} | (\bar{h} S_{\bar{n}})(0) \not{n} i\gamma_{\alpha}^{\perp} \bar{n}_{\beta} (S_{\bar{n}}^{\dagger} g G_s^{\alpha\beta} S_{\bar{n}})(r\bar{n}) (S_{\bar{n}}^{\dagger} h)(0) | \bar{B} \rangle \quad (m_b - 2E_0 \gg \Lambda_{\text{QCD}})$$

A class of models for h_{17} :
$$h_{17}(\omega_1, \mu) = e^{-\frac{\omega_1^2}{2\sigma^2}} \sum_n a_{2n} H_{2n} \left(\frac{\omega_1}{\sigma\sqrt{2}} \right), \quad \sigma < 1 \text{ GeV}$$

 Hermite polynomials

Constraints on moments (e.g.): $\int d\omega_1 h_{17} = \frac{2}{3} \mu_G^2, \quad \int d\omega_1 \omega_1^2 h_{17} = \frac{2}{15} (5m_5 + 3m_6 - 2m_9).$



G+P numerically:
 $\Lambda_{17} \in [-24, 5] \text{ MeV}$ for $m_c = 1.17 \text{ GeV}$.

Factor-of-3 improvement w.r.t. BLNP.

In our code: $\kappa_V = 1.2 \pm 0.3$.
Warning: scheme for m_c !

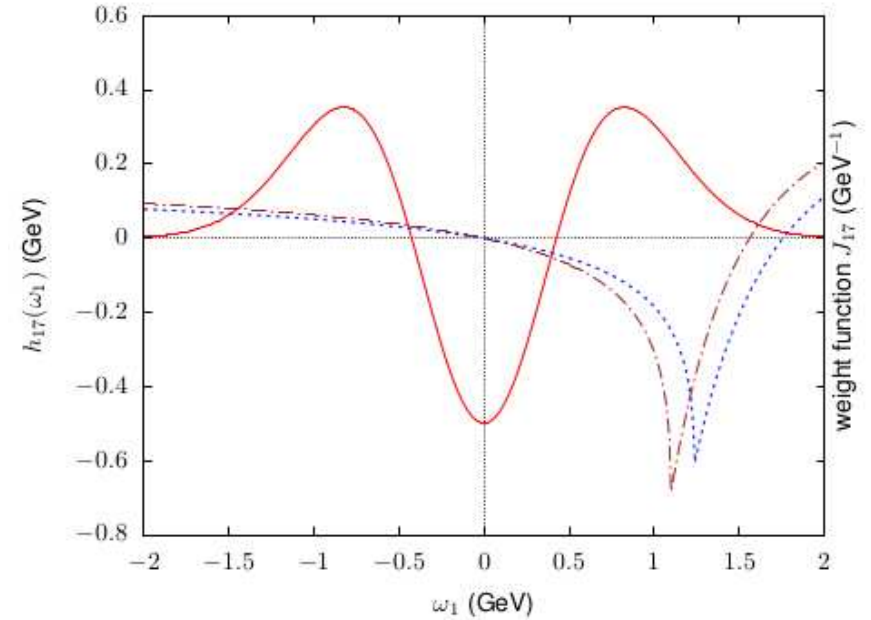
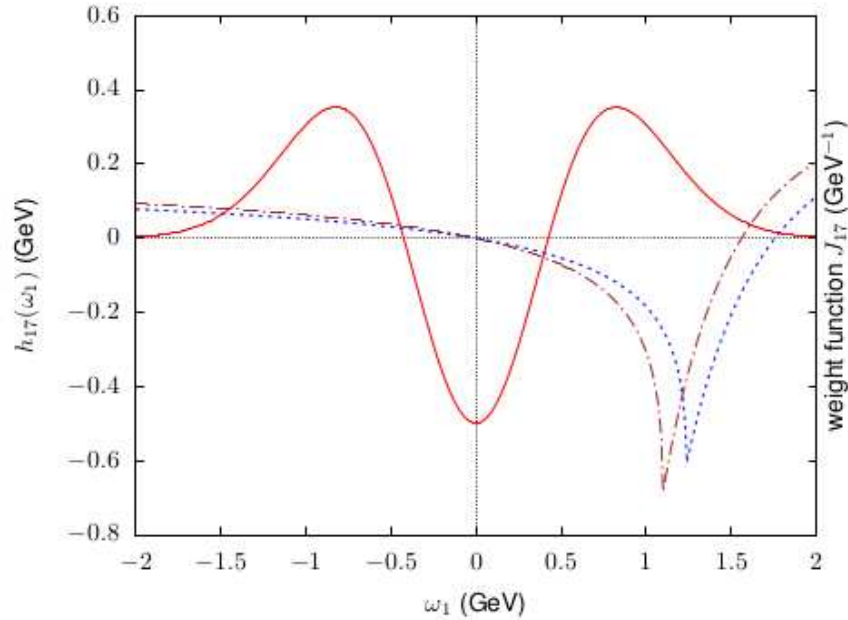
Moment constraints vs. models of h_{17}

M. Benzke, S.J. Lee, M. Neubert, **G. Paz**, arXiv:1003.5012 – only the leading moment included.

A. Gunawardana, **G. Paz**, arXiv:1908.02812 – estimates of the subleading moments from LLSA included.

M. Benzke, T. Hurth, arXiv:2006.00624 – as above but with more generous modeling and partial $1/m_b^2$ corrections.

Plots from the latter article:



Another recent contribution: clarifying the SCET treatment of resolved photons in the Q_8 - Q_8 interference; T. Hurth and R. Szafron, arXiv:2301.01739.

Inclusive determinations of $|V_{cb}|$ with $\mathcal{O}(\alpha_s^3)$ effects.

$$\Gamma(\bar{B} \rightarrow X_c e \bar{\nu}) = \Gamma_0 f(\rho) \left[1 + a_1 \frac{\alpha_s}{\pi} + a_2 \left(\frac{\alpha_s}{\pi} \right)^2 + a_3 \left(\frac{\alpha_s}{\pi} \right)^3 \right. \\ \left. - \left(\frac{1}{2} - p_1 \frac{\alpha_s}{\pi} \right) \frac{\mu_\pi^2}{m_b^2} + \left(g_0 + g_1 \frac{\alpha_s}{\pi} \right) \frac{\mu_G^2}{m_b^2} + d_0 \frac{\rho_D^3}{m_b^3} - g_0 \frac{\rho_{LS}^3}{m_b^3} + \dots \right] \quad (1)$$

$$\Gamma_0 = \frac{G_F^2 m_{b,\text{kin}}^5 |V_{cb}|^2 A_{ew}}{192\pi^3}, \quad f(\rho) = 1 - 8\rho + 8\rho^3 - \rho^4 - 12\rho^2 \ln \rho, \quad \rho = \overline{m}_c^2(\mu_c)/m_{b,\text{kin}}^2.$$

1. Evaluation of a_3 : M. Fael, K. Schönwald, M. Steinhauser, arXiv:2011.13654.
2. Finding $\frac{m_{b,\text{kin}}}{m_{b,\text{pole}}}$ up to $\mathcal{O}(\alpha_s^3)$: M. Fael, K. Schönwald, M. Steinhauser, arXiv:2005.06487, arXiv:2011.11655.
3. Lepton-energy moment fit including $\mathcal{O}(\alpha_s^3)$: M. Bordone, B. Capdevila, P. Gambino, arXiv:2107.00604.
 $\Rightarrow |V_{cb}| = (42.16 \pm 0.51) \times 10^{-3}$
4. Evaluation of several $\overbrace{e\bar{\nu} \text{ invariant mass squared moments}}^{q^2}$ up to $\mathcal{O}(\alpha_s^3)$:
M. Fael, K. Schönwald, M. Steinhauser, arXiv:2205.03410.
5. Extraction of $|V_{cb}|$ from q^2 -moments:
F. Bernlochner, M. Fael, K. Olschewsky, E. Persson, R. van Tonder, K. Vos, M. Welsch, arXiv:2205.10274.
 $\Rightarrow |V_{cb}| = (41.69 \pm 0.63) \times 10^{-3}$
6. ...

Summary

- In the absence (?) of large NP effects in flavour physics, precision calculations are particularly relevant for the SM contributions.
- The measured $B_s \rightarrow \mu^+ \mu^-$ and $\bar{B} \rightarrow X_s \gamma$ branching ratios agree within 1σ with the corresponding SM predictions.
- Further improvement of TH accuracy in $\bar{B} \rightarrow X_s \gamma$ requires getting rid of the interpolation in m_c at $\mathcal{O}(\alpha_s^2)$, as well as resolving the resolved photon issues.
- In the $B_s \rightarrow \mu^+ \mu^-$ case, the main uncertainty comes from $|V_{cb}|$.
- Future determinations of $|V_{cb}|$ from q^2 moments will hopefully lead to further reduction of uncertainties.